



Addis Ababa institute of Technology
School of Electrical and Computer engineering

**Performance Analysis of Precoding Techniques for
5G Massive MIMO and Wireless Systems**

By: Aga Bayou

Advisor: Dr. -Ing. Dereje Hailemariam

Co-advisor: Mr. Amare Kassaw

A Thesis Submitted to the Addis Ababa Institute of Technology,
School of Graduate Studies, Addis Ababa University in Partial Ful-
fillment of the Requirements for the Degree of Masters of Science in
Communication Engineering.

October, 2018
Addis Ababa,
Ethiopia

Addis Ababa University
Addis Ababa institute of Technology
(AAiT)
School of Electrical and computer Engineering

**Performance Analysis of Precoding Techniques for 5G Massive
MIMO and Wireless Systems**

Aga Bayou

Approval by Board of Examiners

Chairman, Dept. Graduate
Committee

Signature

Dr. -Ing. Dereje Hailemariam

Advisor

Signature

Internal Examiner

Signature

External Examiner

Signature

Declaration

I, the undersigned, declare that this thesis is my original work, has not been presented for a degree in this university, and all sources of materials used for the thesis have been fully acknowledged.

Aga Bayou

Name

Signature

Place: Addis Ababa

Date of Submission: _____

This thesis has been submitted for examination with my approval as a university advisor.

Dr. -Ing. Dereje Hailemariam

Advisor's name

Signature

Acknowledgment

Firstly, I would like to express thanks to my supervisor - Dr. -Ing. Dereje Haile-mariam who has supported me throughout my thesis work and sacrifices his valuable times to encouraging me, to work in my own way, and gave me the freedom to explore deep in this study; it would not have been possible to achieve the ultimate target of this study without his valuable helps. He gave me valuable assistances whenever I have a problem with my thesis.

As well, I would like to thank all the member of School of Electrical and Computer Engineering (SECE) specially to division of communication Engineering coordinator Dr. Epherm Teshale for providing such an excellent education and research environment.

I am thankful for all students in Division of Communication Engineering who gave me all knowledge.

Many thanks to the Debre Berhan University for granting me this opportunity, the Electrical and Computer engineering department staff for their supports.

Finally, I am thankful for my family and friends for supporting me and standing beside me at every moment.

Abstract

Due to that wireless technology improvement is ongoing, the numbers of users and applications increase rapidly. Then wireless communications need the high data rate and link reliability at the same time. Future generation wireless communication will have to deal with some core requirements for serving a large number user simultaneously, upholding high throughput for each user, assuring less energy consumption, etc.

In practice, the interuser interference has impact when more users access to the wireless link. Complicated transmission techniques such as interference cancellation should be used to maintain a given desired quality of service. Due to these problems, Massive MIMO with very large antenna arrays are proposed.

Massive MIMO is one of these promising technologies which have introduced the concept of using hundreds or thousands of antennas at the base station and serving tens or hundreds of user simultaneously. A massive number of antennas will help to concentrate the radiated energy into smaller region hence will improve the throughput and energy efficiency of the system.

In this paper, we have investigated the performance of a massive MIMO system utilizing different precoding techniques (e.g. MMSE, ZF, MRT) under Rayleigh fading channel with both complete and incomplete channel state information at the transmitter (CSIT).

Keywords– *MIMO, Massive MIMO, Precoding, MMSE, ZF, MRT, Rayleigh, Capacity, CSIT.*

Contents

Declaration	i
Acknowledgment	ii
Abstract	iii
List of Figures	vii
List of Tables	vii
List of Symbols	viii
List of Abbreviation	ix
1 Motivation and Background	1
1.1 Introduction	1
1.2 Problem Statement	2
1.3 Objective of the thesis	4
1.3.1 General Objective	4
1.3.2 Specific Objective	4
1.4 Literature Review	5
1.5 Methodology	8
1.6 Thesis Contributions and Outline	9
2 Massive MIMO downlink systems	11
2.1 Introduction	11
2.2 Massive MIMO downlink systems	12
2.2.1 Channel Estimation	15
2.2.2 Downlink Data Transmission	20
2.3 Achievable rate	21
2.3.1 Fading channel with perfect CSI at the transmitter	22
2.3.2 Fading channel with no CSI at the transmitter	22

3	Precoding Schemes	24
3.1	Introduction	24
3.2	Downlink Linear Precoding	25
3.2.1	MMSE Precoding	27
3.2.2	Zero forcing (ZF) Precoding	30
3.2.3	MRT Precoding	32
4	Simulation Results and Analysis	36
4.1	Introduction	36
4.2	The Massive MU-MIMO Downlink System over Rayleigh Fading channel with perfect CSI at the transmitter	39
4.2.1	Change in capacity with the increase of the number of Base station antenna	39
4.2.2	Change in capacity with the increase of the number of users	42
4.3	The Massive MU-MIMO Downlink System over Rayleigh Fading channel with no CSI at the transmitter	46
4.3.1	Change in capacity with the increase of the number of Base station antenna under incomplete CSIT	46
4.3.2	Change in capacity with the increase of a number of user .	49
5	Conclusion and Future work	51
5.1	Conclusion	51
5.2	Recommendations for Future Work	52
	References	53

List of Figures

2.1	Downlink M-MIMO system model with M-antennas and K-users [9]	12
2.2	downlink transmission phases	15
3.1	Block diagram of the linear precoders at the BS	25
3.2	Functional block diagram for the single-cell downlink with MMSE processing	29
3.3	Functional block diagram for the single-cell downlink with ZF processing	32
3.4	Functional block diagram for the single-cell downlink with MRT processing	34
4.1	Block diagram of System design	37
4.2	The Spectral Efficiency with different SINR for MMSE, ZF and MRT. $M = 20$, and $K = 10$	40
4.3	Same as Figure 4.1 but with $M = 40$	41
4.4	The spectral efficiency versus the number of antennas over Rayleigh fading channel for MMSE, ZF, and MRT. In this example, $K = 10$ and $SNR = 10$ dB	42
4.5	The spectral efficiency of users with different SNR for MMSE, ZF and MRT over Rayleigh fading channel. In this example, $M = 40$, and $K = 15$	43
4.6	Same as Figure 4.5 but with $K = 25$	44
4.7	The spectral efficiency versus number of users over Rayleigh fading channel for MMSE, ZF, and MRT. $M = 40$ and $SNR = 10$ dB	45
4.8	The achievable rate with different SINR for MMSE, ZF and MRT. $M = 20$, and $K = 10$ under no CSI	46
4.9	Same as Figure 4.8 but with $M = 40$	48
4.10	System capacity with the increase of the number of BS antenna under incomplete CSIT	49
4.11	System capacity with the increase of the number of user under incomplete CSIT	50

List of Tables

4.1	Value of different parameters	38
-----	---	----

List of Symbols

τ_ρ	Pilot coherence interval
h	Scalar h
\mathbf{h}	Vector h
\mathbf{H}	Matrix H
\mathbb{R}	Set of real numbers
\mathbb{C}	Set of complex numbers
$(\cdot)^*$	Complex conjugate
$(\cdot)^T$	Transpose of matrix
$tr(\cdot)$	Trace of square matrix
$(\cdot)^{-1}$	Inverse of matrix
I_N	Identity matrix with size N
$\mathbb{E}[\cdot]$	Mean of the random variable
$\ \cdot\ $	Norm of vector
$ \cdot $	Absolute value
$\mathcal{CN}(0, \sigma^2)$	Circularly symmetric complex Gaussian random variable with zero mean and variance σ^2
$\mathcal{N}(0, \sigma^2)$	Gaussian random variable with zero mean and variance σ^2

List of Abbreviation

CSI	Channel state information
i.i.d.	Independent and identically distributed
LTE	Long Term Evolution
MIMO	Multiple Input Multiple Output
M-MIMO	Massive Multiple Input Multiple Output
MMSE	Minimum mean square error
MRT	Maximum ratio transmission
MSE	Mean square error
MU-MIMO	Multiuser multiple-in and multiple-out
OFDM	Orthogonal frequency division multiplexing
PDF	Probability density function
RZF	Regularized Zero forcing
SDMA	Space division multiple access
SINR	Signal to interference plus noise ratio
SNR	Signal to noise ratio
THP	Tomlinson-Harashima Precoding
ZF	Zero forcing

Chapter 1

Motivation and Background

1.1 Introduction

Performance limitation of wireless network will be at the physical layer, because, fundamentally, the amount of information that can be transferred between two locations is limited by the availability of spectrum, the laws of electromagnetic propagation, and the principles of information theory. There are three basic ways in which the efficiency of a wireless network may be improved [1]:

- Deploying access points more densely;
- Using more spectrum;
- Increasing the spectral efficiency, that is, the number of bits that can be conveyed per second in each unit of bandwidth

While future wireless systems and standards are likely to use an ever-increasing access point density and use new spectral bands, the need for maximizing the spectral efficiency in a given band is never going to vanish.

The use of multiple antennas, also known as multiple-input, multiple-output (MIMO) technology, is viable approach for substantial improvement of spectral efficiency. MIMO technology is logically classified into one of three categories: Point-to-Point MIMO, Multiuser MIMO, and Massive MIMO. This thesis is about Massive MIMO, which arguably will be the ultimate embodiment of MIMO technology.

A massive MIMO is a type of wireless communication system, which uses an antenna array with a large number of antenna, on a scale of few hundreds or thousands [16]. The idea of massive MIMO is for a single base station to serve a multiplicity of terminals using the same time-frequency resources. Effectively, the massive MIMO scenario is obtained from the Point-to-Point MIMO setup by breaking up the K -antenna terminal into multiple autonomous terminals.

The basic concept of massive MIMO is to obtain all the benefits of conventional MIMO but on an enormous scale. Massive MIMO relies on the spatial multiplexing that in turn relies on the base station having sufficient channel information or CSIT. This CSIT is accomplished by having the terminals sending pilots to the BS, based on which BS estimates the channel response to each of the terminals.

Either in uplink or in downlink transmissions, all terminals occupy the full time-frequency resources concurrently. On uplink, the base station has to recover the individual signals transmitted by the terminals. On the downlink, the base station has to ensure that each terminal receives only the signal intended for it. The base station's multiplexing and de-multiplexing signal processing is made possible by utilizing a large number of antennas and by its possession of CSI.

Precoding is one of the ways to improve the transmission using this CSIT. This channel state information at the transmitter (CSIT) can be exploited to enhance the performance of massive MIMO system using various precoding techniques. The precoders adapt the transmission to the channel using CSIT to improve the performance of the system. Precoding also helps to reduce the inter-user interference by focusing the energy on the desired user. Some well-known precoding techniques are, Minimum Mean Square Error (MMSE) precoding, Zero Forcing (ZF) precoding, Maximum Ratio Transmission (MRT) precoding, Regularized Zero Forcing (RZF) precoding, Tomlinson-Harashima (TH) precoding, etc.

In this paper, we have analysed the performance of MMSE, ZF and, MRT precoding in a massive MIMO system considering perfect and imperfect CSIT condition.

1.2 Problem Statement

The major challenges in wireless communication are include spectral efficiency, link reliability, coverage and energy efficiency. This is due to the limited available bandwidth, the fading nature of the propagation channel and the mobility and autonomy of the wireless nodes. The rapid growth in demand for high speed and

high quality multimedia services with diverse QoS requirements is also creating the opportunities and challenges for the system designers. Providing diverse QoS guarantees to the mobile users and various applications is an important objective of next generation wireless networks. However the wireless channel is affected by time-dispersive effects, Doppler and multipath fading, as a result the spectral efficiency of the wireless system is degraded

In order to increase the data rates offered, a simple approach is to increase the allocated bandwidth. This approach is difficult, since the radio-frequency spectrum is scarce resource. Therefore, research over the last years has been focused towards improving spectral efficiency, so that higher data rates can be achieved within a given bandwidth. To improve the spectral efficiency, the conventional scheme and the new massive MIMO cooperative scheme are used adaptively according to channel condition between source and destination.

Massive MIMO (as know as very large MU-MIMO) system has attracted a lot of interest. When the number of antennas increases, the random channel vectors between the users and base station become nearly orthogonal [9]. Other important advantage of massive MU-MIMO systems is that they enable us to reduce the transmitted power. On the uplink, reducing the power of the terminals will save their battery life. On the downlink, much of the electrical base station power is spent by power amplifiers and associated circuits and cooling systems [5]. Hence reducing the RF power would help in cutting the electricity of the base station

Massive MU-MIMO technology is now attracting substantial attention from both academia and industry. This motivates us to work on this topic. Most of the studies considered the uplink performance. Here, we study massive MU-MIMO downlink system with linear precoding. We consider the system performance when the number of antennas and the number of users are large. Our area of interest in this work focus on transmitter precoding impact analysis with respect to achievable sum rates in Massive MIMO systems

In addition to study the massive MU-MIMO system performance, we are inter-

ested in the performance comparisons among linear precoding: Minimum Mean Square Error (MMSE), Zero Forcing (ZF) and Maximum Ratio Transmission (MRT) precoding. Hypothetically, the precoding is known as Space Division Multiple Access. Each linear precoding shows the best performance with each signal power regime. For the comparison between MRT and ZF, MRT gives better performance at low signal to noise ratio (SNR) while ZF performs better at high SNR. MMSE gives the best performance across the entire SNR. These properties are used for improving the performance of massive MU-MIMO in different propagation environments.

1.3 Objective of the thesis

1.3.1 General Objective

To analysis performance of linear precoding algorithms to future massive MIMO wireless systems

1.3.2 Specific Objective

- Review the existing precoding algorithm in massive MIMO
- To analyze the effects in a massive MIMO downlink system with linear precoding and different channel models
- Analysis of the performance of precoders for massive MIMO under;
 - Wireless channel impairments and
 - Various number of receive and transmit antennas.
- We derive linear precoding matrix
- We simulate the channel models with MATLAB software
- We calculate the spectral efficiency to analyze the effect of massive MIMO downlink system over different channel models
- Comparing a reliable and analysis of efficient precoders

1.4 Literature Review

Massive MU-MIMO technology is now attracting substantial attention from both academia and industry. There are different types of research investigated the performance of the precoding techniques in massive MIMO system. Some of the researches conducted on the area of precoding and related to this work are briefly reviewed below.

The first breakthrough to Massive MU-MIMO Downlink TDD Systems with Linear Precoding and Downlink Pilots was made by Thomas Marzetta, et al [2], consider an efficient channel estimation scheme to acquire CSI at each user, called beamforming training scheme. With the beamforming training scheme, the BS precodes the pilot sequences and forwards to all users. Then, based on the received pilots, each user uses minimum mean-square error channel estimation to estimate the effective channel gains. Then they derive a lower bound on the capacity for maximum-ratio transmission and zero-forcing precoding techniques to evaluate the spectral efficiency taking into account the spectral efficiency loss associated with the transmission of the downlink pilots. They also hinted the potential benefits of massive MIMO.

Because of its advantage over conventional point-to-point communications as discussed above, the massive MIMO concept has gained great attention in recent research. Md. Mahfuzur Rahman and Dr.Md. Abu Bakar Siddiqui [3] investigated the BER performance of massive MIMO system with increasing number of BS antenna, users, and SINR. They compared Spectral efficiency and BER performance of ZF, MMSE precoding under Perfect CSIT and Imperfect CSIT. It was shown that performance of a massive MIMO system utilizing different precoding techniques (MMSE, ZF, MRT) under Rayleigh fading channel with both complete and incomplete channel state information at the transmitter (CSIT) are investigated. In their's work, three types of hypothetical assumption are considered to assume the missing information of the CSIT and analysed the performance of the precoders using these assumptions

In [4], Adil Israr, Zahid Rauf, Jan Muhammad and Faisal Khan compares the performance of Massive MIMO downlink including linear precoding is evaluated. The achievable rate and the downlink transmit power of ZF and MRT precoding techniques are derived, analyzed and compared under the same conditions and assumptions. Their scenarios considered to investigate these performance parameters are when the ratio of BS antennas and number of users is large, ZF is better than MRT while when the ratio is quite small it makes MRT better than ZF for the same conditions

In [5], the art of novel low-complexity high-performance precoding algorithms with both linear and non-linear processing strategies are explored. It proposes Block diagonalization (BD) linear precoding type based to reduce the computational complexity and improve the performance of BD-type precoding algorithms. Two categories of low complexity linear precoding are proposed to reduce the computational complexity and improve the performance of BD-type precoding algorithms. One is based on multiple LQ decompositions and lattice reductions. The other one is based on a channel inversion technique, QR decompositions, and lattice reductions to decouple the MU-MIMO channel into equivalent SU-MIMO channels. Both of the two proposed precoding algorithms can achieve a comparable sum-rate performance as BD-type precoding algorithms, substantial bit error rate (BER) performance gains, and a simplified receiver structure, while requiring a much lower complexity

Tomlinson-Harashima precoding (THP) is a prominent nonlinear processing technique employed at the transmit side is investigated and its performance strongly depend on the ordering of the precoded symbols. They propose a multi-branch THP (MB-THP) scheme and algorithms that employ multiple transmit processing and ordering strategies along with a selection scheme to mitigate interference in MU-MIMO systems. Two types of multi-branch THP (MB-THP) structures are proposed. The first one employs a decentralized strategy with diagonal weighted filters at the receivers of the users and the second uses a diagonal weighted filter at the transmitter. The MB-MMSE-THP algorithms are also derived based on an extended system model with the aid of an LQ decomposition, which is much simpler compared to the conventional MMSE-THP algorithms. They show that a

better BER performance can be achieved by the proposed MB-MMSE-THP precoder with a small computational complexity increase

In [8] shows a performance analysis of a large multi-user MIMO downlink system over frequency selective fast fading channel under Rician distribution was analyzed using ZF, MMSE and MRT precoding. The performance has been investigated in terms of BER and throughput. In this work a perfect feedback channels was considered. The performance analysis of linear precoding for MIMO system based Imperfections CSI is investigated by [10]. The result showed that linear precoding provides significant gains even with imperfect CSI.

The work in [9] analyzed the performance of multiple inputs multiple output orthogonal space time blocks coding MIMO-OSTBC over frequency selective fading channel using Bit Error Rate (BER) and spectral efficiency (SE) as performance measures. The results showed that, as SNR increases, the spectral efficiency increases while the BER reduces for different antenna configurations. The authors in [13] analyzed OSTBC of MIMO systems for both perfect and imperfect CSI.

In reference [11] the authors suggested the most favourable types of beamforming techniques that can be deployed in massive MIMO systems and to clarify the importance of beamforming techniques in massive MIMO systems for eliminating and resolving many technical hitches that massive MIMO system implementation faces. The authors aim at evaluating of optimal beamforming techniques that are used in wireless communication systems to determine which techniques are more suitable for deployment in massive MIMO systems to improve system throughput and reduce intra- and inter-cell interference. They suggested an optimal beamforming technique that can provide the highest performance in massive MIMO systems, satisfying the requirements of next-generation wireless communication systems.

1.5 Methodology

In this study, related secondary sources of data such as different books in LTE, 3GPP standardization documents, previous researcher's studies, different Institute of Electrical and Electronics Engineers (IEEE) articles, development in 5G cellular technology in general and basics of massive MIMO in particular.

Based on the inputs retrieved from review of related literatures and the statement of the problem in mind, the methodology of this study is designed as follows;

System design

- Outline work flows for spectral efficiency of the system;
- Setup target network requirements in terms of spectral efficiency;
- Prepare a mathematical model for calculating the capacity of the system;
 - Generating channel,
 - Defining precoding matrices with their power constraints,
 - calculating SINR for each user,
 - Calculating the achievable rate of each user,
 - Calculating total capacity of all users hence total capacity of the system and finally taking an average of all realization (in this paper 1000) to find the final system capacity
- Identify all input parameters for simulation

Simulations:

- Outline simulation work flow
- Perform target network capacity prediction simulations;
- Simulate target network to evaluate the capacity.

Result Analysis & Interpretations:

- Perform spectral efficiency (capacity) evaluation analysis whether the target network requirement achieved or not.

1.6 Thesis Contributions and Outline

In all the literatures seen so far in Section 1.3, precoding has been investigated at various levels. However, some of the differences in the previous work and the current work are underlined in the following points.

- A Massive-MIMO system using linear precoding system is presented. The system throughput expression and the achievable rate of a user over Rayleigh fading channels are derived. With different linear precoding scheme, the M-MIMO achieve better performance. In this work, If the channel state information at the transmitter (CSIT) is not perfect, the missing information is obtained using statistical properties and there is noise in the channel. since the pilot signals(known at both ends of the link and from which the base station estimates the channels) propagate through the uplink channel, So in order to get CSI at downlink, the base station performs a de-spreading operation by correlating the received signals with each of pilot sequences. During de-spreading operation the noise is also spread. But in most of literatures [2, 3, 8, 13], three types of hypothetical assumption (Ones Assumption, Mean Assumption and Random Assumption) and there is no noise in the channel are considered to assume the missing information of the CSIT and analysed the performance of the precoders.

- We consider only linear processing at downlink(MMSE, ZF and MRT) since number of base station antenna is typically much larger than number of terminals in massive MIMO. Moreover, zero-forcing and maximum-ratio themselves tend to be optimal under high and low SINR conditions respectively.

While there are somewhat better performing alternatives: nonlinear processing, which increase mathematical complexity and suitable when number of base station and terminals are nearly equal, and suitably optimized block diagonalization(BD) linear precoding type, which uses LQ and QR decom-

position to decouple MU-MIMO channel into SU-MIMO to reduce computational complexity and to improve performances on the downlink [5]

- The spectral efficiency for M-MIMO with given target of SINR are compared.
- The complexities analyze of M-MIMO with perfect CSIT and imperfect CSIT condition linear precoding are considered

Rest of the paper is organized as;

- Chapter 2, Provides the background studies of massive MIMO system, Fading channel, Channel Estimation, short description of perfect and imperfect CSIT and shows the equation for the achievable rate of a user in M-MIMO system.
- Chapter 3, Describes the precoding techniques used in this work.
- Chapter 4, Provides the simulation results and discussion of M-MIMO for system including the linear precoding
- Chapter 5, the conclusion and suggestions for future work were presented

Chapter 2

Massive MIMO downlink systems

2.1 Introduction

A Massive MIMO system refers to the system where the base station communicates with several users simultaneously. The base station and the user can be equipped with multiple antennas. The M-MIMO system enables many parallel communications in the same time and frequency resource that called Space Division Multiple Access (SDMA).

Advantages of Massive-MIMO systems:

- Increased data rate, due to base station is equipped with many antennas, it sends the independent data streams to many users simultaneously (multiplexing gain).
- Link reliability, due to that antennas generate a lot of communication paths that the radio signal can propagate over (diversity gain).
- Improving the energy efficiency, due to that base station is able to focus its transmission power into the spatial direction where each user is located (array gain).

The three fundamental features render Massive MIMO scalable with respect to the number of base station antennas, M are;

- Only the base station learns channel state information (CSI), H
- M is typically much larger than K
- Simple linear signal processing is used both on the uplink and on the downlink

This chapter will describe the principle of Massive MIMO downlink system, which includes; Rayleigh fading channel, channel estimation, downlink data transmission and achievable rate

2.2 Massive MIMO downlink systems

We consider the case of a single base station that simultaneously serves K terminals. We call the area where the terminals are located a cell, and refer to the corresponding scenario as single-cell, emphasizing the fact that there is no inter-cell interference to account for.

Figure 2.1 illustrates the basic downlink Massive MIMO setup. Each base station is equipped with a large number of antennas, M , and serves a cell with a large number of terminals, K through Rayleigh fading channels, and that the channels will stay constant during a coherence interval of T symbols. The terminals typically (and throughout this thesis) have a single antenna each.

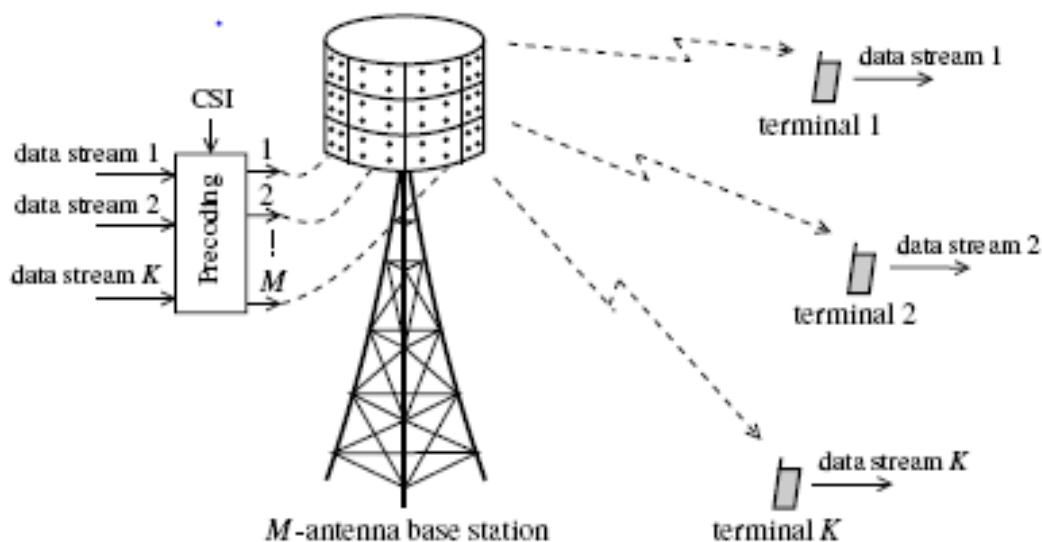


Figure 2.1: Downlink M-MIMO system model with M -antennas and K -users [9]

Let h_k^m be the channel gain between the k^{th} terminal and the m^{th} base station antenna. We will assume that the base station antennas are configured in a compact array, so that the paths between a given terminal and all base station antennas are affected by the same large-scale fading, but by different small-scale fading.

$$h_k^m = \sqrt{\beta_k} g_k^m, \quad k = 1, \dots, K, m = 1, \dots, M, \quad (2.1)$$

where β_k is a large-scale fading coefficient that depends on k but not on m , and g_k^m

represents the effect of small-scale fading.

We let H be a matrix that comprises the channel gains between all terminals and all base station antennas [3]

$$H = \begin{bmatrix} h_1^1 & h_2^1 & \cdot & \cdot & \cdot & h_K^1 \\ h_1^2 & h_2^2 & \cdot & \cdot & \cdot & h_K^2 \\ \cdot & \cdot & \cdot & & & \cdot \\ \cdot & \cdot & & \cdot & & \cdot \\ \cdot & \cdot & & & \cdot & \cdot \\ h_1^M & h_2^M & \cdot & \cdot & \cdot & h_K^M \end{bmatrix} \quad (2.2)$$

Throughout all performance analyses, we will assume that the small-scale fading is Rayleigh and independent between the antennas and the terminals, so that h_k^m are i.i.d. $\mathcal{CN}(0, 1)$ random variables.

Rayleigh Fading Channel

In the wireless communication, it is difficult to find the exact channel properties because of multipath propagation in each environment. Nonetheless, channel models are used for analyzing system performance. One of the channel models, which is used for modeling the channel fading, is a Rayleigh fading channel.

The model assumption is that the summation of many statistically independent reflected and scattered paths with random amplitudes is an independent and identically distributed (i.i.d) complex Gaussian random variable. The element of the channel matrix can be written in a complex number form as [25].

$$h_k^m = c + jd \quad (2.3)$$

The joint probability density function (*PDF*) can be written as

$$f_{c,d}(c,d) = \frac{1}{2\pi\sigma^2} e^{-\frac{c^2 + d^2}{2\sigma^2}} \quad (2.4)$$

Expressing h_k^m in polar form we obtain

$$h_m^k = r e^{j\theta} \quad (2.5)$$

Where $r = \sqrt{c^2 + d^2}$, $\theta = \arctan\left(\frac{d}{c}\right)$

From polar form, we can write the joint *PDF* of R and θ by

$$f_{R,\theta}(r,\theta) = \frac{r}{2\pi\sigma^2} e^{-\frac{r^2}{2\sigma^2}} \quad (2.6)$$

By integration with θ we obtain the *PDF* of R as

$$P_R(r) = \frac{r}{\sigma^2} e^{-\frac{r^2}{2\sigma^2}} \quad (2.7)$$

The *PDF* of R is same as Rayleigh distributed. By above properties, Rayleigh fading channel can be described in terms of amplitude and phase.

The channel coefficient of complex Rayleigh fading is generated by two Gaussian random variables where each variable has zero mean and variance σ . Each Gaussian random variable is put in the real part and imaginary part. Then, the channel coefficient of Rayleigh fading channel is given by;

$$h_{Rayleigh} = c + jd \quad (2.8)$$

Where $c \in \mathcal{N}(0, \sigma)$ and $d \in \mathcal{N}(0, \sigma)$

2.2.1 Channel Estimation

An additional consequence of using large numbers of antennas is that the required signal processing and resource allocation simplifies, owing to a phenomenon known as channel hardening. The significance of channel hardening is that effects of small-scale fading and frequency dependence disappear when M is large. Furthermore, channel hardening renders channel estimation at the terminals, and the associated transmission of downlink pilots

Typically, the channel estimation is done on the downlink. More precisely, each user estimates the channel using pilot sequences transmitted from the base station, and then it feedbacks this CSI to the base station. This channel estimation overhead will be proportional to the number of base station antennas. Therefore, with massive MIMO system, this is very inefficient. Thus, here we assume that the channel is estimated at the base station via uplink pilots, assuming channel reciprocity. Since Uplink and downlink channels are reciprocal in TDD because it uses the same frequency spectrum for the uplink and downlink transmissions but with different time slots. M is large in massive MIMO therefore, TDD operation is preferable in Massive MIMO

The downlink and uplink channels can not be perfectly reciprocal in practice because of hardware chains mismatch. But with proper calibration [13], this non-reciprocity can be removed. In this work, it is assumed that the hardware chain calibration is perfect.

The downlink transmission will occur in two phases: Training phase and Downlink data transmission phase



Figure 2.2: downlink transmission phases

τ_p is the coherence duration used for the training phase. In the training phase,

the base station estimates the channel state information (CSI) from K users based on the received pilot sequences in the uplink. The base station uses this CSI and linear precoding schemes to process the transmit data.

A wideband channel can be decomposed into coherence intervals of duration T_c seconds and bandwidth B_c Hz. Every such interval offers $\tau_c = B_c T_c$ independent uses of a frequency-flat channel. Illustrates the three activities that occupy each coherence interval: uplink data transmission, uplink pilot transmission, and downlink data transmission. In every coherence interval, the terminals use τ_ρ of the τ_c available samples to transmit pilots that are known at both ends of the link, and from which the base station estimates the channels.

Each user is assigned an orthogonal pilot sequence of τ_ρ symbols where $\tau_\rho \geq K$. Any set of orthogonal pilots with the same energies yield the same performance. The significance of τ_ρ is to quantify how much energy each terminal spends on pilots in each coherence interval. In principle, any τ_ρ samples in the uplink part of the coherence interval can be used for pilots. In practice, transmitters are typically peak-power limited, so constant-modulus signals, such as orthogonal sine waves, make ideal pilots. We assign the k^{th} terminal a pilot sequence denoted by a $\tau_\rho \times 1$ vector ϕ_k , which is the k^{th} column of a $\tau_\rho \times K$ unitary matrix, such that $\tau_\rho \geq K$ and

$$\Phi^H \Phi = I_K \quad (2.9)$$

Collectively, the terminals then transmit a $K \times \tau_\rho$ signal

$$X_\rho = \sqrt{\tau_\rho} \Phi^H, \quad (2.10)$$

which is normalized so that each terminal expends a total energy that is equal to the duration of the pilot sequence,

$$\tau_\rho \phi_k^H \phi_k = \tau_\rho \quad (2.11)$$

The $M \times \tau_\rho$ received pilot matrix at the base station is given by [1];

$$Y_\rho = \sqrt{\rho_\rho} H \Phi^T + N_\rho \quad (2.12)$$

Where $\Phi \in \tau_\rho \times K$ is the pilot sequence used by K users satisfying $\Phi\Phi^H = I_K$; $N_\rho \in \mathbb{C}^{M \times \tau}$ is the additive noise at the base station; $\rho_\rho = \tau_\rho \rho_u$ where ρ_u is the transmitted power of each user.

The base station performs a de-spreading operation by correlating the received signals with each of the K pilot sequences. This is equivalent to right-multiplying the received signal matrix by the matrix of pilots, yielding

$$Y'_\rho = Y_\rho \Phi \quad (2.13)$$

$$Y'_\rho = \sqrt{\rho_\rho} H + N'_\rho \quad (2.14)$$

$$\text{Where } N'_\rho = N_\rho \Phi^*$$

Let y_k and n_k be the k^{th} columns of Y'_ρ and N'_ρ respectively

$$y'_{\rho,k} = \sqrt{\rho_\rho} h_k + n'_k \quad (2.15)$$

No information is lost in the de-spreading operation because multiplication of the received pilot signal by any vector in the orthogonal complement of Φ would only result in still another noise matrix that is statistically independent of both H and N'_ρ

Assuming that the base station uses **MMSE channel estimation**, After de-spreading, the base station has a noisy version (2.15) of the channel matrix. Under the assumption of independent Rayleigh fading, the elements of the channel matrix and the noise matrix are statistically independent. Hence, channel estimation decouples over both the base station antennas and the terminals, and it is sufficient to consider only the $(m, k)^{\text{th}}$ component of (2.15),

$$\left[Y'_\rho \right]_k^m = \sqrt{\rho_\rho} h_k^m + \left[N'_\rho \right]_k^m \quad (2.16)$$

By assumption, the large-scale fading coefficients are known, so the prior distribution of h_k^m , $\mathcal{CN}(0, \beta_k)$, is also known. The MMSE estimator is [7]

$$\hat{h}_k^m = E \{ h_k^m | Y_\rho \} = E \{ h_k^m | Y'_\rho \} = \frac{\sqrt{\rho_\rho} \beta_k}{1 + \rho_\rho \beta_k} \left[Y'_\rho \right]_k^m \quad (2.17)$$

The mean-square of the channel estimate is denoted by γ_k and given by

$$\gamma_k = E \{ |\hat{h}_k^m|^2 \} = \frac{\rho_\rho \beta_k^2}{1 + \rho_\rho \beta_k} \quad (2.18)$$

In (2.18), is the same for all m , since the channels for each of the antennas are statistically identical. The channel estimation error is denoted by

$$\tilde{h}_k^m = \hat{h}_k^m - h_k^m \quad (2.19)$$

and the mean-square estimation error is

$$E \{ |\tilde{h}_k^m|^2 \} = \frac{\beta_k}{1 + \rho_\rho \beta_k} = \beta_k - \gamma_k \quad (2.20)$$

The channel estimation error is uncorrelated with both the channel estimate and the pilot signal,

$$E \{ \tilde{h}_k^m (\hat{h}_k^m)^* \} = 0, \quad (2.21)$$

$$E \{ \tilde{h}_k^m [Y_p']_{mk}^* \} = 0 \quad (2.22)$$

The estimation error \tilde{h}_k^m and the estimate \hat{h}_k^m are jointly Gaussian distributed, so the fact that they are uncorrelated implies that they are also statistically independent.

The estimator defined by (2.17) is the same for every antenna index, as are the mean-square channel estimate (2.18) and the mean-square error (2.20). The estimate of the channel to the k^{th} terminal is denoted by an $M \times 1$ vector $\hat{h}_k = [\hat{h}_k^1, \hat{h}_k^2, \dots, \hat{h}_k^M]^T$, which, to facilitate subsequent derivations, is expressed in normalized form as follows:

$$\hat{h}_k = \sqrt{\gamma_k} z_k \quad (2.23)$$

Where the components of z_k are i.i.d. $\mathcal{CN}(0, 1)$. Using (2.23), we write the estimate of the complete channel matrix to the K terminals, H , in normalized form as

$$\hat{H} = Z D \frac{1}{\gamma} \quad (2.24)$$

Where $\gamma = [\gamma_1, \dots, \gamma_K]^T$ is a $K \times 1$ vector of mean-square channel estimates, and Z is an $M \times K$ matrix whose entries are i.i.d. $\mathcal{CN}(0, 1)$.

2.2.1.1 Perfect and Imperfect CSIT

Perfect CSIT means that the transmitter knows all the components of H instantaneously and without errors ($\beta_k = \gamma_k$). In an ideal scenario like this, the performance of the system can be increased very much using the CSIT.

It is in fact, impossible to achieve perfect CSIT because the transmission should be instantaneous, the precision of the electronics should be infinite, and some other hypothesis that in the reality are impossible. To be more realistic it can be considered that the CSI is incomplete. It means that only a part of the channel is unknown. It can be due to some user not knowing its channel. Then a whole row of H is missing. Or due to some resources constraints in the system that doesn't let know a specific amount of information of the channel. It can also be originated because an error on the obtainment of the CSI or a quantification error. An example of the imperfect CSIT could be like this [3],

$$H = \begin{bmatrix} h_1^1 & h_2^1 & h_3^1 & h_4^1 & h_5^1 & h_6^1 \\ h_1^2 & h_2^2 & h_3^2 & h_4^2 & h_5^2 & h_6^2 \\ \theta & \theta & h_3^3 & \theta & \theta & \theta \\ h_1^4 & h_2^4 & h_3^4 & h_4^4 & h_5^4 & h_6^4 \\ \theta & \theta & \theta & \theta & \theta & h_6^5 \end{bmatrix} \quad (2.25)$$

In this example, it can be seen that the users 1, 2 and 4 transmit all the CSI but users 3 and 5 just transmit the information only for the path from antenna 3 and 6 respectively.

2.2.1.2 Assumption of Channel State Information

If the channel state information at the transmitter (CSIT) is not perfect, there are two options, first is not to perform any precoding and using old transmission using

other techniques rather than MIMO techniques, second is the missing values of the CSIT can be assumed. The missing information can be obtained using statistical properties

2.2.2 Downlink Data Transmission

The base station has to ensure that each terminal receives only the signal intended for it. The base station's multiplexing and de-multiplexing signal processing is made possible by utilizing a large number of antennas and by its possession of CSI to process the signals before transmitting them to K users.

Downlink data transmission entails a linear precoding operation that combines the message bearing symbols with the downlink channel estimates to create the actual signals that the array transmits. The m^{th} antenna transmits a weighted symbol [7],

$$x_m = \sqrt{\eta_m} q_m \quad (2.26)$$

$$x = D_{\eta}^{\frac{1}{2}} q \quad (2.27)$$

Where η_m is a power control coefficient that satisfies $0 \leq \eta_m \leq 1$. The symbols $\{q_m\}$ have zero mean and unit variance, and they are uncorrelated,

$$E \{qq^H\} = I_M \quad (2.28)$$

The signal received vector at the K user terminals can be expressed as:

$$y = \sqrt{\rho_{dl}} H^T x + n \quad (2.29)$$

Where $y \in \mathbb{C}^{M \times 1}$ is the received signal vector at the k^{th} user ($k = 1, 2, \dots, K$), $x \in \mathbb{C}^{M \times 1}$ is the signal vector transmitted at the base station such that $E[||x||^2] = 1$; $n \in \mathcal{CN}(0, \sigma^2 I)$ is the noise vector with I , being the identity matrix. The superscript T symbolizes the transpose and ρ_{dl} is the average SINR.

2.3 Achievable rate

In Massive MIMO, after appropriate signal processing, the effective channel associated with each of the terminals is a scalar point-to-point channel. Each time this channel is used, it takes a (complex-valued) scalar input symbol x and delivers a (complex-valued) output signal y . The action of the channel is characterized by the conditional probability distribution of y given x .

The system performance can be defined by several methods. One of method, to quantify the system performance, is the achievable rate. The achievable rate is followed by Shannon theorem. This theory tells the maximum rate, which the transmitter can transmit over the channel.

To communicate a message over a point-to-point scalar channel, the transmitter maps the message onto a sequence of symbols $\{x_n\}$, and the receiver recovers the message from the sequence of samples $\{y_n\}$. The effective number of bits conveyed per transmitted symbol, denoted by R , is called the rate and is measured in bits per channel use (*bpcu*). Recall that a waveform contained in a time-frequency space of bandwidth B Hz and time-duration T seconds can be described by BT samples. Hence, transmitting a waveform with bandwidth B Hz and time-duration T seconds is equivalent to transmitting BT symbols $\{x_n\}$. Therefore, the rate R is usually termed spectral efficiency and measured in bits per second per Hertz (*b/s/Hz*).

Consideration of net spectral efficiency alone according to the rigorous Shannon theory suggests the optimality of a rough parity between number of transmitter antenna (M) and number of receiver antenna (K) in conventional Multiuser MIMO: further growth of M only yields logarithmically increasing throughputs while incurring linearly increasing amounts of time spent on training [9]. Massive MIMO represents a clean break from conventional Multiuser MIMO. Measures are taken such that one operates farther from the Shannon limit, but paradoxically achieves much better performance than any conventional Multiuser MIMO system

Throughout this work, motivated by the channel coding theorem, we will use such capacity bounds as the primary performance metric. These capacity bounds can typically be approached closely in practice by using state-of-the-art channel coding techniques. Some key results on capacity and capacity bounds for point-to-point scalar channels that will be needed for the performance analysis in precoding are discussed below.

2.3.1 Fading channel with perfect CSI at the transmitter

A fading channel with Gaussian noise n and a gain h that is perfectly known to the transmitter. Here,

$$y = \sqrt{\rho} H^T x + n \quad (2.30)$$

x and n are independent, and, in addition, h is a random variable that represents the fading channel gain and which is independent of x and n . New independent realizations of h and n are drawn for each transmitted symbol x . The distribution of h can be arbitrary. Equation (2.30) applies; $E\{|x|\}^2 \leq 1$, $E\{n\} = 0$, and $\text{Var}\{n\} = 1$. The capacity is

$$C = \log(1 + \rho |H^T|^2) \quad (2.31)$$

2.3.2 Fading channel with no CSI at the transmitter

We next extend the previous model to the case of an unknown channel gain. The signal x and the noise n are uncorrelated, but not necessarily independent. Neither the transmitter, nor the receiver knows H . Also, H and x are independent; however, no assumption is made on the statistical relation between H and n .

To obtain a simple capacity bound, we rewrite the expression for y as follows [1]:

$$y = \sqrt{\rho} E\{H^T\}x + \sqrt{\rho} (H^T - E\{H^T\})x + n \quad (2.32)$$

The receiver's lack of knowledge about H is captured by the second term $\sqrt{\rho} (H^T - E\{H^T\})x$. A direct calculation shows that the second and third terms of (2.32) are mutually uncorrelated, and uncorrelated with x . Considering the two last terms of (2.32) as *effective noise*, the channel in (2.32) is, with appropriate normalization, equivalent

to the model in deterministic channel with Additive Non-Gaussian Noise

$$C \geq \log_2 \left(1 + \frac{\rho |E\{H^T\}|^2}{\rho \text{Var}\{H^T\} + 1} \right) \quad (2.33)$$

The bound in (2.33) is mainly useful when h fluctuates only slightly around its expected value $E\{H^T\}$, so that $\text{Var}\{H^T\}$ is small. This will be the case in many of the derivations of capacity bounds for Massive MIMO. The train of reasoning can be summarized as follows:

- Owing to the linear beamforming, each terminal sees a scalar channel with unknown gain h , and additive uncorrelated effective noise that comprises receiver noise and interference.
- The effect of the lack of knowledge of h , captured in the deviation $h - E\{h\}$, is treated as additional uncorrelated effective noise. By virtue of channel hardening, while h is random and unknown, it fluctuates only slightly around $E\{h\}$ so this additional effective noise is small.
- The variances of all effective noise terms depend only on second- and fourth-order moments of Gaussian random variables, and hence can be computed in closed form.

Chapter 3

Precoding Schemes

3.1 Introduction

Transmit precoding (beamforming) is a versatile technique for signal transmission from an array of M antennas to one or multiple users. In wireless communications, the goal is to increase the signal power at the intended user and reduce interference to non-intended users. A high signal power is achieved by transmitting the same data signal from all antennas, but with different amplitudes and phases, such that the signal components add coherently at the user. Low interference is accomplished by making the signal components add destructively at non-intended users. This corresponds mathematically to designing beamforming vectors (that describe the amplitudes and phases) to have large inner products with the vectors describing the intended channels and small inner products with non-intended user channels.

Since transmit precoding focuses the signal energy at certain places, less energy arrives to other places. This allows for so-called space-division multiple access (SDMA), where K spatially separated users are served simultaneously. One beamforming vector is assigned to each user and can be matched to its channel. Unfortunately, the finite number of transmit antennas only provides a limited amount of spatial directivity, which means that there are energy leakages between the users which act as interference.

While it is fairly easy to design a beamforming vector that maximizes the signal power at the intended user, it is difficult to strike a perfect balance between maximizing the signal power and minimizing the interference leakage.

There are basically two techniques of precoding: linear types, e.g. ZF, MMSE, MF and non-linear precoding, e.g. THP, VP, etc

3.2 Downlink Linear Precoding

Linear precoding is a transmitter-based precoding scheme for compensating for the multipath interfering effect of the communication channel. By means of linear precoding techniques in the downlink, the BS transmits linearly precoded information data with signal vector x , which is predicated for the K users by [1]

$$x = PD_{\eta}^{\frac{1}{2}}q = \sum_{k=1}^K \sqrt{\eta_k} p_k q_k \quad (3.1)$$

Where $P \in \mathbb{C}^{M \times K}$ designates the precoding matrix, $q \triangleq [q_1, q_2, \dots]^H$ denotes the signal vector which encloses the data symbols for the K user, D_{η} represents the normalization constant which has been chosen subject to power constraint $E\{\|x\|^2\} \leq 1$. A block diagram of the linear precoder at the BS is shown in Figure (3.1)

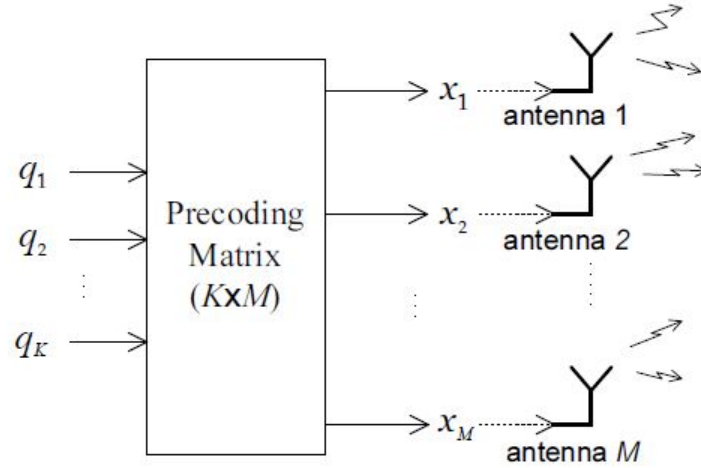


Figure 3.1: Block diagram of the linear precoders at the BS

[13]

The expected power that is used for the k^{th} terminal is

$$E\left\{\|\sqrt{\eta_k} p_k q_k\|^2\right\} = \eta_k E\left\{\|p_k\|^2\right\} \quad (3.2)$$

Therefore, the transmitter vector y can be written as,

$$y = \sqrt{\rho_{dl}} H^T P q + n \quad (3.3)$$

The base station does not know the actual channel, but it does know the channel estimate that it derived from the uplink pilots. Within (3.3), we replace H by $\hat{H} - \tilde{H}$, where $\tilde{H} = \hat{H} - H$ is a matrix of channel estimation errors, and in turn we replace the channel estimate by its normalized version (2.24). This yields

$$\begin{aligned} y &= \sqrt{\rho_{dl}} (\hat{H} - \tilde{H})^T x + n \\ &= \sqrt{\rho_{dl}} \hat{H}^T x + (n - \sqrt{\rho_{dl}} \tilde{H}^T x) \\ &= \sqrt{\rho_{dl}} \hat{H}^T P D_{\eta}^{\frac{1}{2}} q + (n - \sqrt{\rho_{dl}} \tilde{H}^T x) \end{aligned} \quad (3.4)$$

Which expresses the received signal as if the transmitted signals passed through a known channel followed by the addition of the quantities in parentheses that constitute effective noise. The effective noise is uncorrelated with the desired signal term because the receiver noise n is independent of everything else, and the channel estimation error \tilde{H} and the channel estimate \hat{H} are uncorrelated

The signal received by the k^{th} terminal is

$$y_k = \sqrt{\rho_{dl}} \hat{h} P D_{\eta}^{\frac{1}{2}} + n_k - \sqrt{\rho_{dl}} \tilde{h}^T x \quad (3.5)$$

The three terms in (3.5) are mutually uncorrelated. For subsequent use, we evaluate the variance of the sum of the last two terms,

$$\begin{aligned} \text{var} \{ n_k - \sqrt{\rho_{dl}} \tilde{h}^T x \} &= 1 + \rho_{dl} E \{ x^H \tilde{h}_k^* \tilde{h}_k^H x \} \\ &= 1 + \rho_{dl} (\beta_k - \gamma_k) E \{ \|x\|^2 \} \end{aligned} \quad (3.6)$$

which, significantly, depends only on the total radiated power.

3.2.1 MMSE Precoding

MMSE precoding is the optimal linear precoding in massive MIMO downlink system. This technique is generated by the mean square error (MSE) method. Owing to average power at each transmitted antenna is constrained, Lagrangian optimization method is used for obtaining this precoder. Firstly, we start to consider the MSE of the signal. The MSE can be written as [20];

$$\varepsilon = \mathbb{E} \left[\|\alpha y - x\|^2 \right] \quad (3.7)$$

We find the precoding matrix P_{MMSE} and α to minimize the MSE under the average power constrain D_η . This is stated mathematically as

$$\begin{aligned} [P_{MMSE}, \alpha] &= \arg \min_{P_{MMSE}, \alpha} (\varepsilon) \\ s.t. \sum_{k=1}^K \mathbb{E} \left[\|q_k\|^2 \right] &= D_\eta \end{aligned} \quad (3.8)$$

To solve the optimization problem, the Lagrangian method is used for this problem [7]. Then,

$$\mathcal{L}(P_{MMSE}, \alpha, \lambda) = \varepsilon - \lambda \text{tr}(x^H x - D_\eta) \quad (3.9)$$

Where $\lambda \in \mathbb{R}$ is the Lagrangian factor

In order to find P_{MMSE} and λ to minimize the MSE, we take derivatives with respect to P_{MMSE} , and λ . Firstly we take derivatives with respect to P_{MMSE}

$$\frac{\partial \mathcal{L}(P_{MMSE}, \lambda)}{\partial P_{MMSE}} = 2\alpha^2 H^* H^T W - 2\lambda P_{MMSE} - 2\alpha Z^* = 0 \quad (3.10)$$

Therefore,

$$P_{MMSE}(\mu) = \frac{1}{\alpha} H^* (H^T H^* + \mu I_K)^{-1} \quad (3.11)$$

Where we replace $-\frac{\lambda}{\alpha^2}$ by $\mu \times \mathbb{R}$. Owing to the power constrain in (3.8), α can be

represented as a function of $\hat{\mathbf{A}}_{\dagger}$. More precisely,

$$\alpha(\mu) = \sqrt{\frac{\text{tr}(H^T H^* (H^T H^* + \mu I_K)^{-2})}{D_\eta}} \quad (3.12)$$

Therefore, the constrained optimization problem with respect to P_{MMSE} and α can be reduced to an unconstrained optimization problem with respect to μ

$$\hat{\mu} = \min_{\mu} \mathcal{E}(P_{MMSE}(\mu)) \quad (3.13)$$

Therefore, the constrained optimization problem with respect to P_{MMSE} can be reduced to an unconstrained optimization problem with respect to μ . We take a derivative with respect to μ equal to zero and we can obtain

$$\hat{\mu} = \frac{\text{tr}(I_K)}{D_\eta} = \frac{K}{D_\eta} \quad (3.14)$$

Substituting (3.14) into (3.13) the optimal MMSE precoding W is given by

$$P_{MMSE} = H^* \left(H^T H^* + \frac{K}{D_\eta} I_K \right)^{-1} \quad (3.15)$$

Let y_k^{MMSE} , x_k , and n_k be the k^{th} elements of $K \times 1$ vectors y , x , and n respectively and we define the k^{th} column of P_{MMSE} as

$$p_k^{MMSE} = H^* \Lambda_k \quad (3.16)$$

Where Λ_k is the k^{th} column of $H^* \left(H^T H^* + \frac{K}{D_\eta} I_K \right)^{-1}$. From (3.16), the received vector of k^{th} user with MMSE is given by

$$y_k^{MMSE} = \frac{1}{\alpha} h_k^T H^* \Lambda_k q_k + \frac{1}{\alpha} \sum_{i=1, i \neq k}^K H_k^T H^* \Lambda_i q_i + n_k \quad (3.17)$$

The resulting capacity is

$$C_{inst.,k}^{MMSE,dl} = \mathbb{E} \left[\log_2 \left(1 + SINR_k^{MMSE,dl} \right) \right] \quad (3.18)$$

Where

$$SINR_k^{MMSE,dl} = \frac{|h_k^T H^* \Lambda_k|^2}{\sum_{i=1, i \neq k}^K |h_k^T H^* \Lambda_i|^2 + 1} \quad (3.19)$$

Block diagram below shows the corresponding functional block.

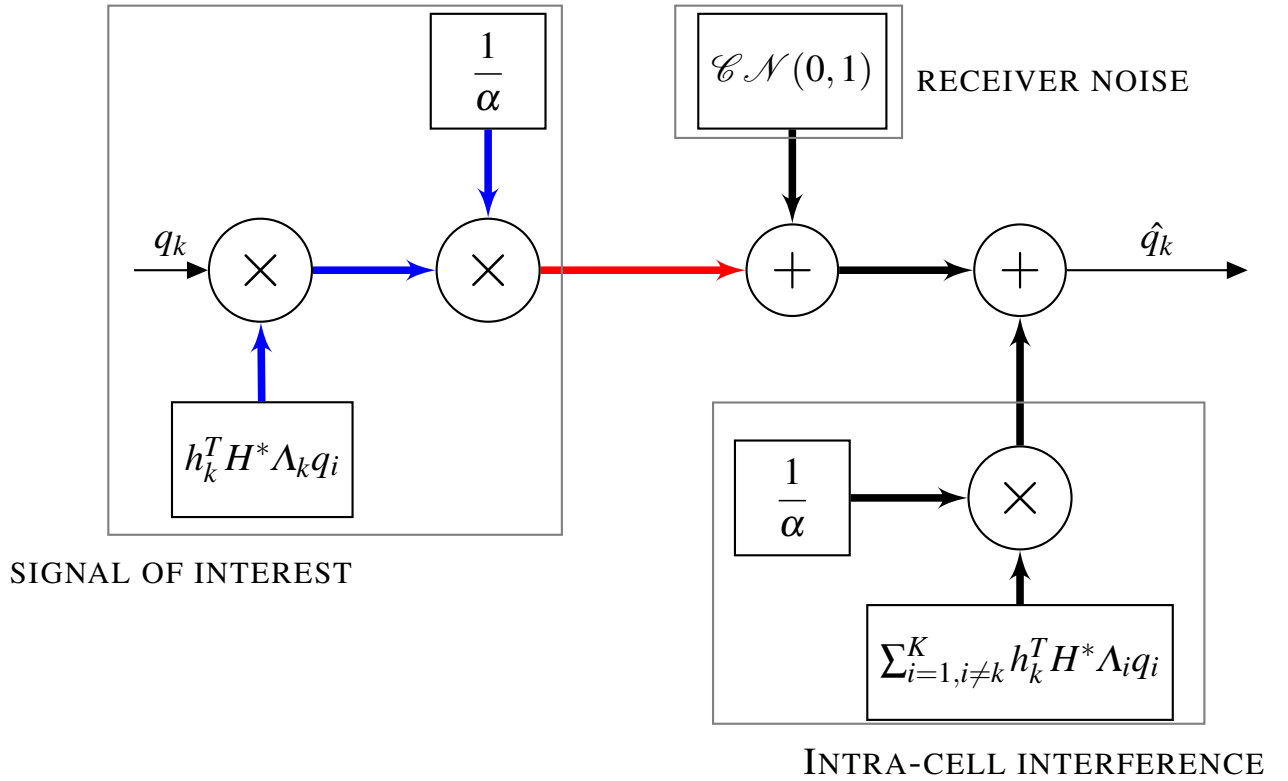


Figure 3.2: Functional block diagram for the single-cell downlink with MMSE processing

Interpretation of the Effective SINR

The effective SINR expression in (3.26) as follows:

- The frequency dependence of the channels disappears from the formulation. This is consistent with the fact that the coherent beamforming gain as well

as the effects of intra-cell interference arise from the combined action of many antennas.

- The numerator represents the coherent beamforming gain for the signal designated for the k^{th} terminal
- The denominator comprises noise and intra-cell interference

3.2.2 Zero forcing (ZF) Precoding

The ZF precoding is a well-known MIMO precoding method due to its low complexity nature and ZF precoding can be implemented without having any prior knowledge of noise statistics. With ZF, the multi-user interference is completely nulled out by projecting each stream onto the orthogonal complement of the interuser interference. ZF approaches *MMSE* when $D_\eta \rightarrow \infty$. Therefore, from (3.15), P_{ZF} can be expressed as

$$P_{ZF} = \frac{1}{\alpha} H^* (H^T H^*)^{-1} \quad (3.20)$$

Where $\alpha = \sqrt{\frac{\text{tr}(BB^H)}{D_\eta}}$, $B = H^* (H^T H^*)^{-1}$

$$E \left\{ \left\| \sqrt{\eta_k} p_k q_k \right\|^2 \right\} = \eta_k \quad (3.21)$$

The substitution of (3.20) into (3.3) gives the following received signal vector:

$$y^{ZF} = \frac{1}{\alpha} H^* (H^T H^*)^{-1} q + n \quad (3.22)$$

Let y_k , x_k , and n_k be the k^{th} elements of $K \times 1$ vectors y , x , and n respectively and we define the k^{th} column of P_{ZF} as

$$p_{ZF} = H^* g_k \quad (3.23)$$

Where g_k is the k^{th} column of $(H^T H^*)^{-1}$.

$$y_k^{ZF} = \frac{1}{\alpha} h_k^T H^* g_k q_k + \frac{1}{\alpha} \sum_{i=1, i \neq k}^K h_k^T H^* g_i q_i + n_k \quad (3.24)$$

Equation (3.24) expresses the received signal in terms of a deterministic gain $\sqrt{\rho_{dl} \gamma_k \eta_k}$ multiplied by the symbol of interest, q_k , plus uncorrelated effective noise.

The resulting capacity is

$$C_{inst.,k}^{zf,dl} = \mathbb{E} \left[\log_2 \left(1 + SINR_k^{zf,dl} \right) \right] \quad (3.25)$$

Where the effective SINR is given by

$$SINR_k^{zf,dl} = \frac{\frac{1}{\alpha^2} |h_k^T H^* g_k|^2}{\frac{1}{\alpha^2} \sum_{i=1, i \neq k}^K |h_k^T H^* g_i|^2 + 1} \quad (3.26)$$

Interpretation of the Effective SINR

The effective SINR expression in (3.26) as follows:

- The frequency dependence of the channels disappears from the formulation, and only the large-scale fading coefficients appear. This is consistent with the fact that the coherent beamforming gain as well as the effects of intra-cell interference arise from the combined action of many antennas.
- The numerator represents the coherent beamforming gain for the signal designated for the k^{th} terminal:
- The denominator comprises noise and intra-cell interference, whose magnitude is independent of M :
 - The term "1" corresponds to receiver noise.
 - The remaining term, which is convenient to think of as intra-cell interference, represents the effects of channel estimation errors

- The interference arrives only by the path to the k^{th} terminal, and is proportional only to the total radiated power, i.e., the sum of the power control coefficients.

Block diagram below shows the corresponding functional block. The numerators of the SINRs have identical form. For the downlink case, the effective noise depends only the channel estimation error for the k^{th} terminal weighted by the total transmitted power, because the k^{th} terminal receives power only through its own channel.

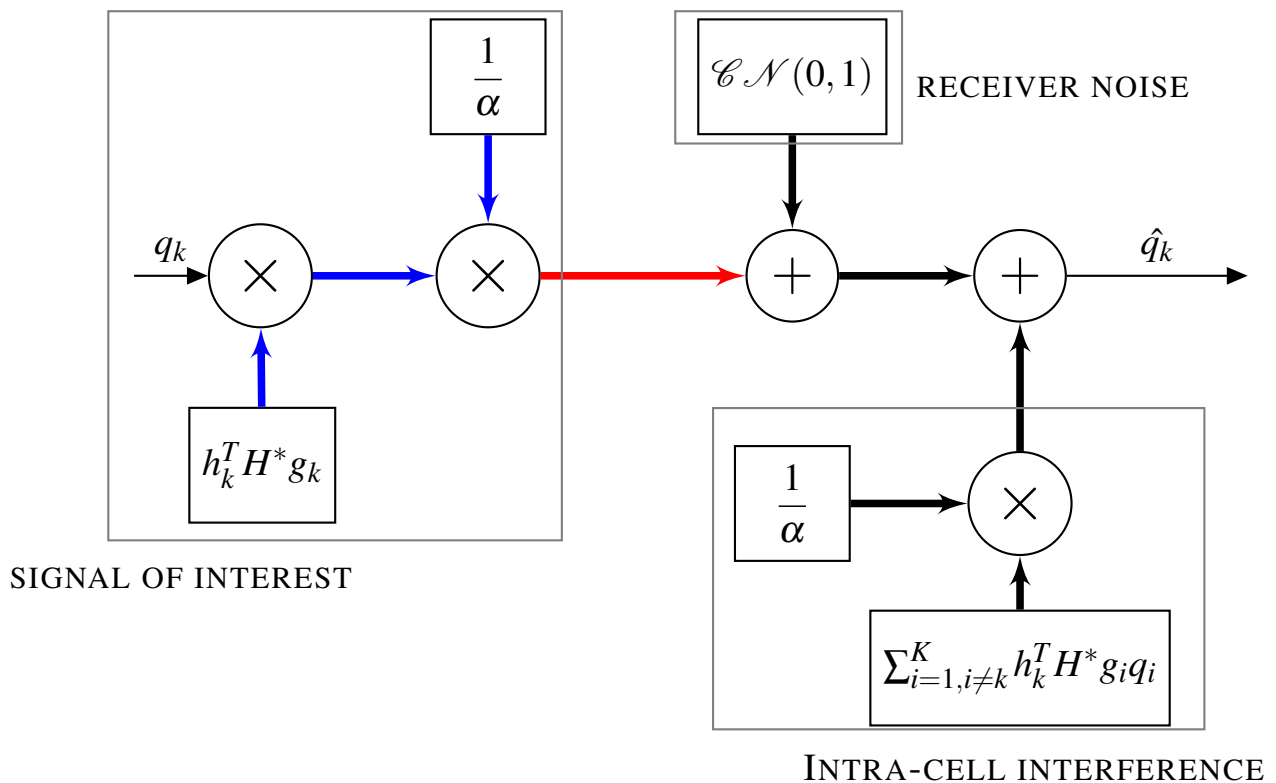


Figure 3.3: Functional block diagram for the single-cell downlink with ZF processing

3.2.3 MRT Precoding

The MRT is also one of the simplest and oldest precoding techniques applied to maximize the received SNR at the user mobile terminal. Works well in the M-MIMO system where the base station radiates low signal power to the users.

MRT approaches $MMSE$ when $D_\eta \rightarrow 0$ Hence, from (3.15), P_{MRT} can be expressed as

$$P_{MRT} = \frac{1}{\alpha} H^* \quad (3.27)$$

$$\text{Where } \alpha = \sqrt{\frac{\text{tr}(BB^H)}{D_\eta}}, B = Z^*$$

As in the case of zero-forcing, the expected power expended on the k^{th} terminal is equal to η_k

The substitution of (3.27) into (3.4) gives the received signals,

$$y^{MRT} = \frac{1}{\alpha} H^T H^* q + n \quad (3.28)$$

Let y_k , x_k , and n_k be the k^{th} elements of $K \times 1$ vectors y , x , and n respectively and we define the k^{th} column of P_{MRT} as

$$p_{MRT} = h_k^* \quad (3.29)$$

The k^{th} received signal is

$$y_k^{MRT} = \frac{1}{\alpha} h_k^T h_k^* q_k + \frac{1}{\alpha} \sum_{i=1, i \neq k}^K h_k^T h_i q_i + n_k \quad (3.30)$$

The resulting capacity bound is

$$C_{inst.,k}^{MRT,dl} = \mathbb{E} \left[\log_2 \left(1 + SINR_k^{MRT,dl} \right) \right] \quad (3.31)$$

Where the effective SINR is given by

$$SINR_k^{zf,dl} = \frac{\frac{1}{\alpha^2} \|h_k\|^4}{\frac{1}{\alpha^2} \sum_{i=1, i \neq k}^K |h_k^T h_i^*|^2 + 1} \quad (3.32)$$

The coherent beamforming gain is equal to $\frac{1}{\alpha^2} \|h_k\|^4$, which is larger than the zero-forcing gain.

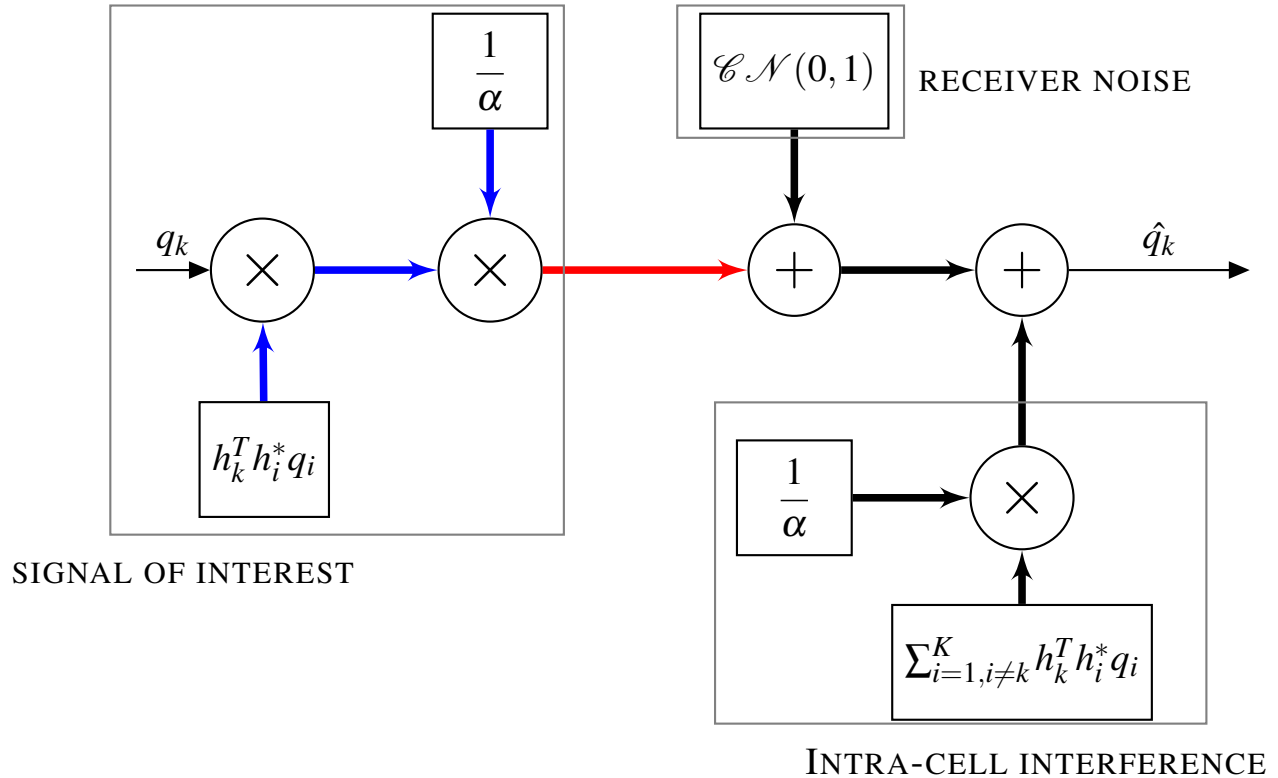


Figure 3.4: Functional block diagram for the single-cell downlink with MRT processing

Interpretation of the Effective SINR Expressions

The functional block diagrams and the companion effective SINR expressions provide considerable intuitive insight:

- The frequency dependence of the channels disappears from the formulation. This is consistent with the fact that the coherent beamforming gain as well as the effects of intra-cell interference arise from the combined action of many antennas.
- The numerator represents the coherent beamforming gain for the signal designated for the k^{th} terminal:

- The factors $\frac{1}{\alpha^2} \|h_k\|^4$ represent the effective strengths of the channel between the base station and the k^{th} terminal
- Only the k^{th} power control coefficient, η_k , affects the gain.
- The denominator comprises noise and intra-cell interference
 - The term "1" corresponds to receiver noise.
 - The remaining term, which is convenient to think of as intra-cell interference, represents the effects of channel estimation errors, channel non-orthogonality and beamforming gain uncertainty as well.
 - The interference arrives only by the path to the k^{th} terminal, and is proportional only to the total radiated power, i.e., the sum of the power control coefficients.

Chapter 4

Simulation Results and Analysis

4.1 Introduction

This chapter will present the simulation results, and massive MU-MIMO system

We have done the performance analysis simulation for four different cases such as,

Case 1. Change in capacity with the increase of the number of Base station antenna having complete CSI.

Case 2. Change in capacity with the increase of the number of users having complete CSI.

Case 3. Change in capacity with the increase of a number of base station antenna having incomplete CSI. Lastly,

Case 4. Change in capacity with the increase of a number of user having incomplete CSI.

However, the limitation of models are that the number of users K is not greater than the number of antennas M . All results are shown in terms of;

- The achievable rate versus Signal-to-Interference Ratio (SINR)
- The achievable rate versus the number of antenna arrays
- The achievable rate versus the number of users

The simulation algorithm analysis is done in below block diagram steps.

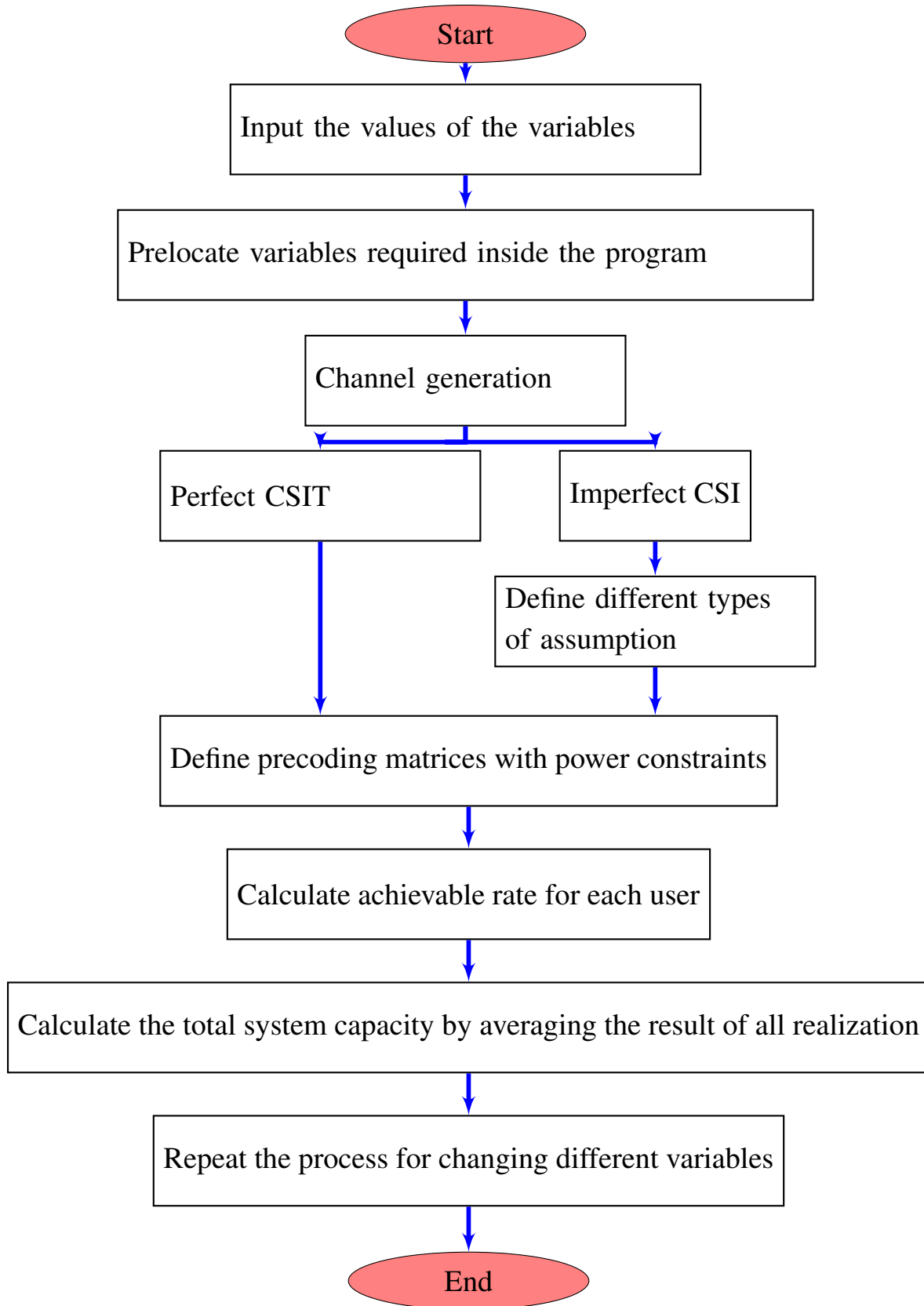


Figure 4.1: Block diagram of System design

Values of different parameters used for simulation is given in Table below. In 4G mobile technology, assures the high mobility with high level speed of data rates and high capacity IP based services and application are standardized. Our parameter is related with advanced LTE standardized [22]

For fixed point, Assuming a uniform distribution of input signal values, the quantization noise is a uniformly distributed random signal with a peak-to-peak amplitude of one quantization level. For q -bit integers with equal distance between quantization levels (uniform quantization), the SINR is approximately

$$SINR_{db} = 6.02q \quad (4.1)$$

This relationship is the origin of statements like "16-bit audio has a dynamic range of 96 dB"

Floating point numbers provide a way to trade off signal-to-noise ratio for an increase in dynamic range. For q bit floating-point numbers, with $q - m$ bits in the mantissa and m bits in the exponent [12]:

$$SINR_{db} = 6.02(q - m) \quad (4.2)$$

The dynamic range is much larger than fixed-point, but at a cost of a worse signal-to-noise ratio. This makes floating-point preferable in situations where the dynamic range is large or unpredictable. Fixed-point's simpler implementations can be used with no signal quality disadvantage in systems where dynamic range is less than $6.02m$. The very large dynamic range of floating-point can be a disadvantage, since it requires more forethought in designing algorithms

Table 4.1: Value of different parameters

4.2. The Massive MU-MIMO Downlink System over Rayleigh Fading channel with perfect CSI at the transmitter

Parameter	Values	Remarks
SINR (When Fixed)	10dB	LTE signal strength range
SINR (Range)	-20 to 20dB	LTE signal strength range
Number of BS Antenna (Fixed)	$M = 20$ and 40	Variable
Range of BS antenna (When varied)	20 to 100	Variable
Number of users (Fixed)	10	Variable
Number of users(Varied)	15 and 25	Variable
Number of realization	1000	Variable

4.2 The Massive MU-MIMO Downlink System over Rayleigh Fading channel with perfect CSI at the transmitter

4.2.1 Change in capacity with the increase of the number of Base station antenna

We choose the number of users $K = 10$. We change the number of antennas from 20 to 100. We set up the BS power from -20 to 20 dB.

Figure 4.2 shows the achievable rate of users across the entire SINR range. This system consists of the number of antennas $M = 20$ and the number of users $K = 10$. The results show that MRT gives the better performance at low SINR. On the other sides, ZF gives better performance at high SINR. MMSE performs the best achievable rate across SINR range.

4.2. The Massive MU-MIMO Downlink System over Rayleigh Fading channel with perfect CSI at the transmitter

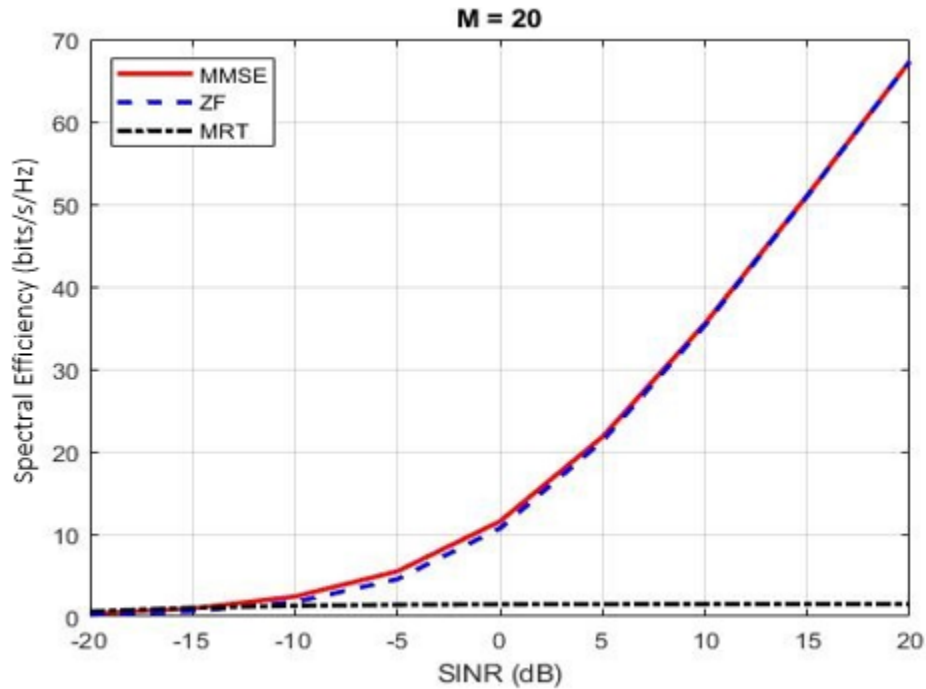


Figure 4.2: The Spectral Efficiency with different SINR for MMSE, ZF and MRT. $M = 20$, and $K = 10$

Figure 4.3 shows the achievable rate of users when we increase the number of antennas from 20 to 40. All results show that the system performance is improved. The achievable rates of MMSE, ZF, and MRT are increased by increasing the number of antennas. Corresponding to the results in Figure 4.2, MMSE gives the highest achievable rate to users. For comparison between ZF and MRT, ZF still gives the better performance at high SNR while MRT performs the higher rate at low SNR. We observe that a point, where ZF performance is better than MRT, is moved from -10 to -13 dB SINR. Increasing the number of antennas makes ZF able to be used at low SINR.

4.2. The Massive MU-MIMO Downlink System over Rayleigh Fading channel with perfect CSI at the transmitter

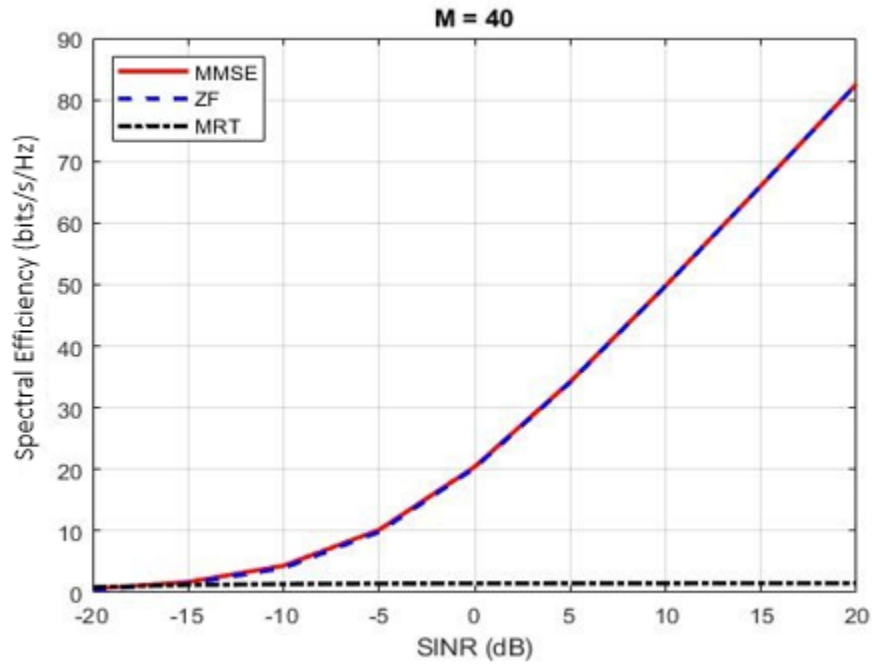


Figure 4.3: Same as Figure 4.1 but with $M = 40$

Figure 4.4 shows the spectral efficiency versus the number of antennas at 10 dB SINR. Corresponding to the results in Figures 4.2 and 4.3, Figure 4.4 shows that all spectral efficiencies with linear precoding increased significantly by increasing the number of antennas. For example, the spectral efficiency with ZF increases

4.2. The Massive MU-MIMO Downlink System over Rayleigh Fading channel with perfect CSI at the transmitter

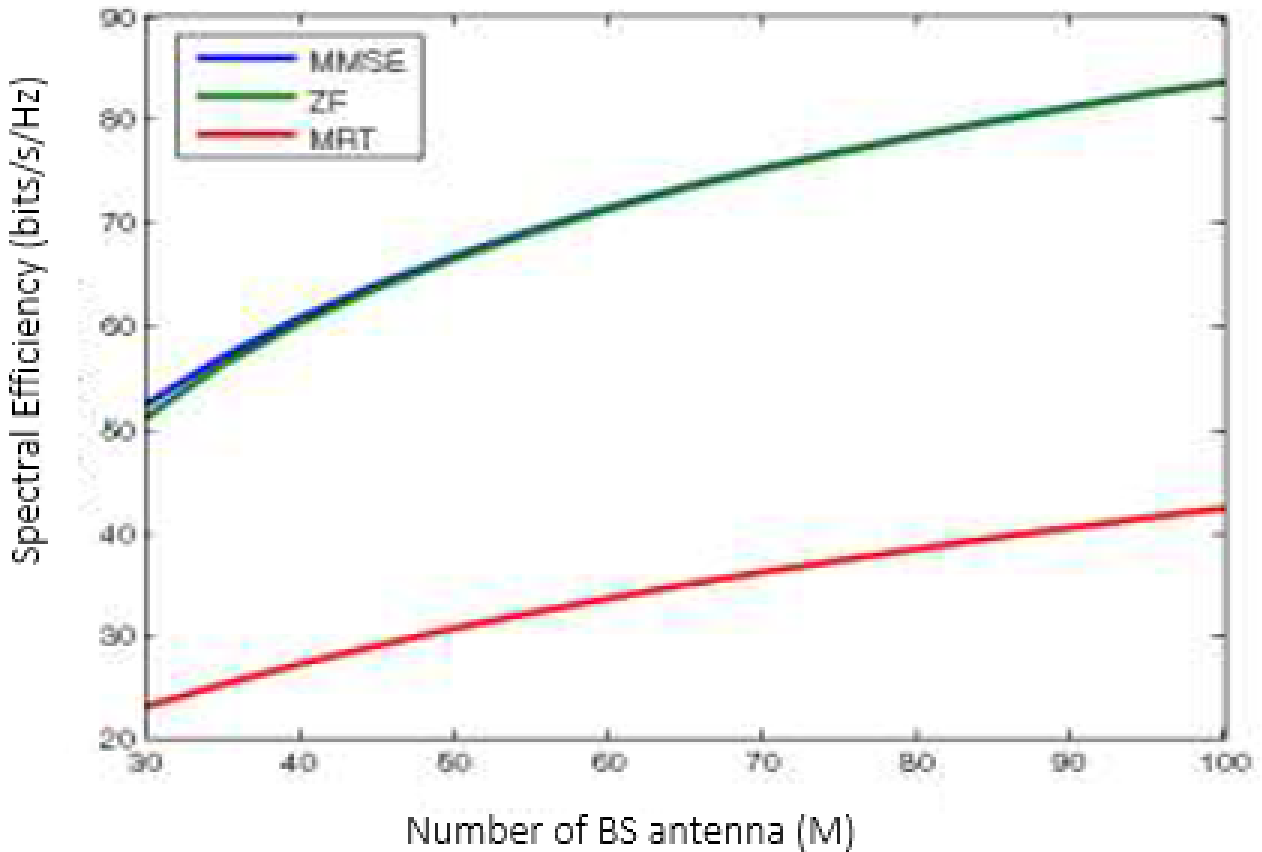


Figure 4.4: The spectral efficiency versus the number of antennas over Rayleigh fading channel for MMSE, ZF, and MRT. In this example, $K = 10$ and $\text{SNR} = 10$ dB

4.2.2 Change in capacity with the increase of the number of users

We fix the number of antennas M and increase the number of users K , which $K < M$. In this scenario, we consider $M = 40$ and $K = 15$ and 25 respectively. We choose SNR from -20 to 20 dB. All results are shown in figures below.

4.2. The Massive MU-MIMO Downlink System over Rayleigh Fading channel with perfect CSI at the transmitter

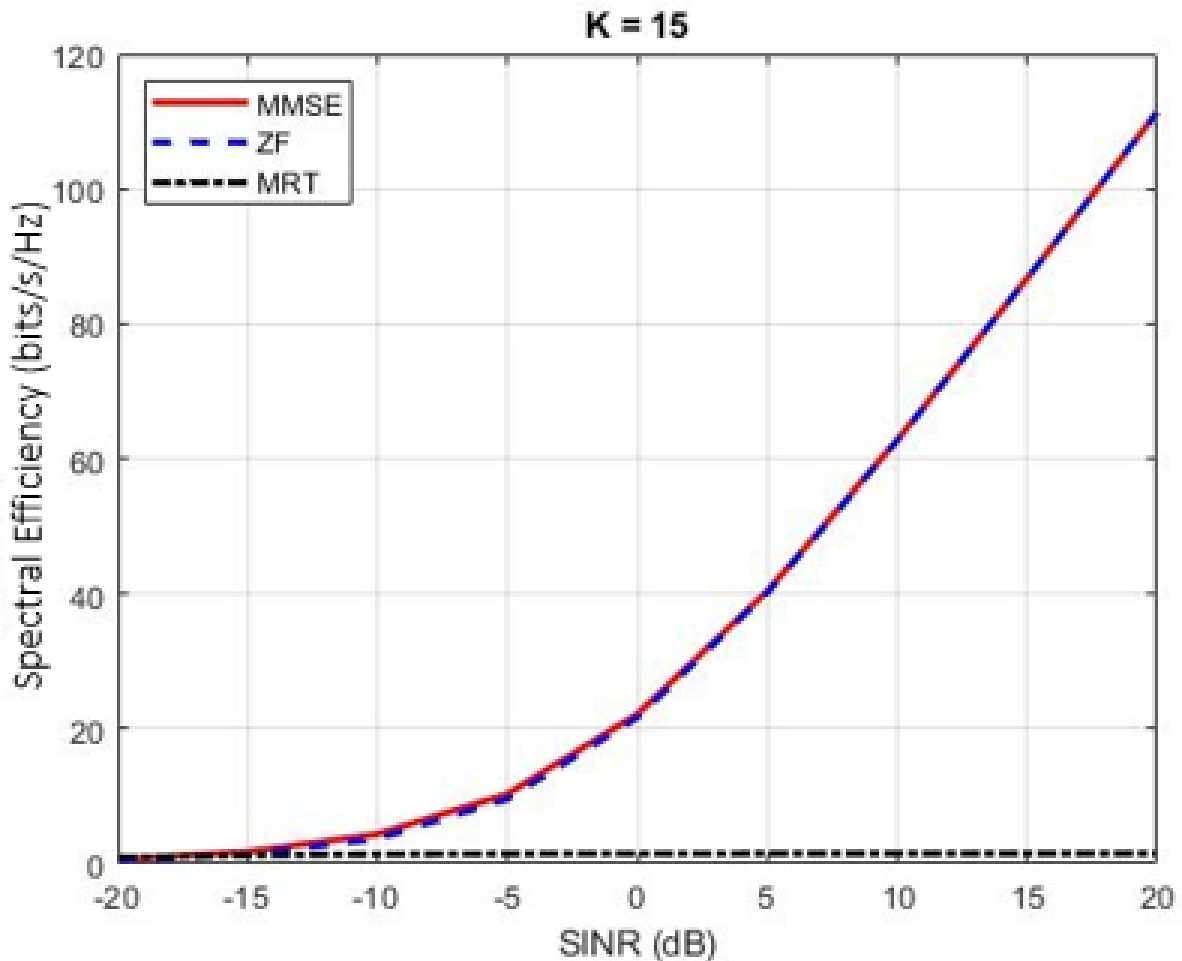


Figure 4.5: The spectral efficiency of users with different SNR for MMSE, ZF and MRT over Rayleigh fading channel. In this example, $M = 40$, and $K = 15$

Figure 4.6 shows that the achievable rate of user 1 with $M = 40$ serving $K = 15$. From the comparison between Figure 4.5 and Figure 4.6, massive MU-MIMO downlink system performance decreases significantly due to inter-user interference. All achievable rates of user 1 with linear precoding are reduced around 0.5 bits/s/Hz at 20 dB SNR.

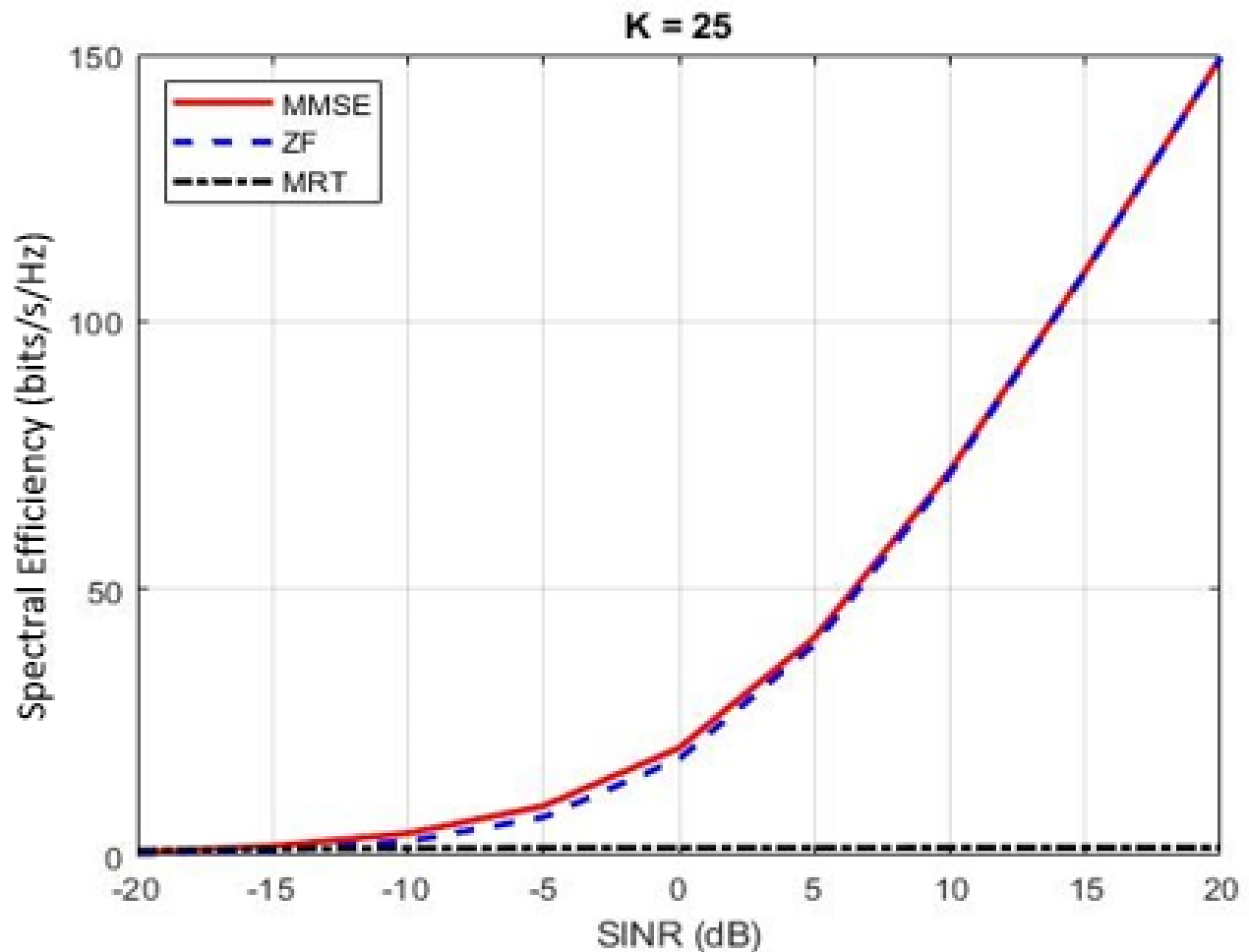


Figure 4.6: Same as Figure 4.5 but with $K = 25$.

Although increasing the number of users reduces the achievable rate of user 1, MMSE gives the highest data rate. At low SNR, MRT performs the higher rate while ZF give the better performance in term of the achievable rate at the high SNR. Notice that the gap between MMSE and ZF is extended. Moreover, the SNR range where the achievable rate of user 1 with MRT is greater than one with ZF, is extended further.

In Figure 4.7, the results show the spectral efficiency versus the number of users at 10 dB SNR. The spectral efficiency with MMSE increases rapidly until $K = 25$. When $K > 25$, increasing the spectral efficiency is very slow. After $K > 30$, the spectral efficiency is decreased slightly. As the result, $K = 30$ is an optimal number with MMSE.

4.2. The Massive MU-MIMO Downlink System over Rayleigh Fading channel with perfect CSI at the transmitter

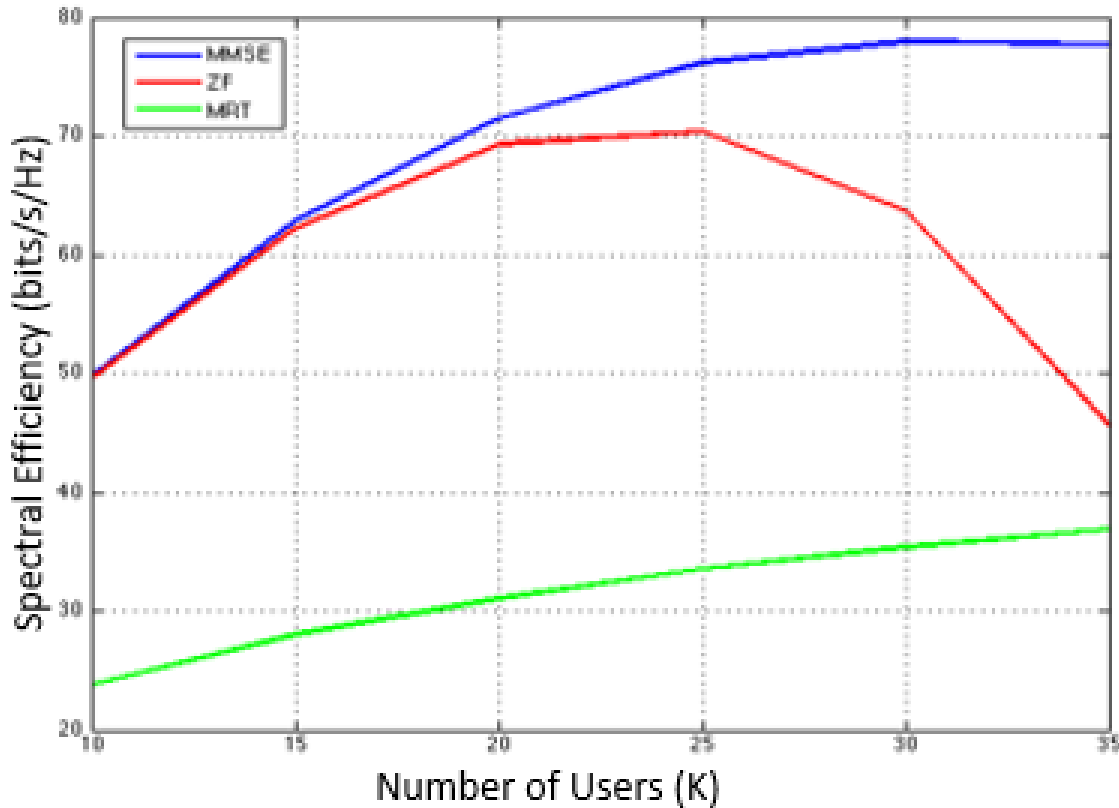


Figure 4.7: The spectral efficiency versus number of users over Rayleigh fading channel for MMSE, ZF, and MRT. $M = 40$ and $\text{SNR} = 10$ dB

According to MMSE result, the spectral efficiency with ZF increases quickly by increasing the users. Until $K > 25$, the spectral efficiency is dropped rapidly. With ZF, the optimal number of users is around 25 for a massive MIMO downlink system over Rayleigh fading channel with $M = 40$.

On the other hand, the spectral efficiency versus the number of users with MRT increases slowly although the number of users K increases. However, the spectral efficiency with MRT is less than MMSE and ZF.

4.3 The Massive MU-MIMO Downlink System over Rayleigh Fading channel with no CSI at the transmitter

4.3.1 Change in capacity with the increase of the number of Base station antenna under incomplete CSIT

In Figure 4.8, the CSIT of the system is considered incomplete, and variance = 0.3 is applied. Due to imperfect CSIT, the capacity of all precoder falls than the capacity with perfect CSIT.

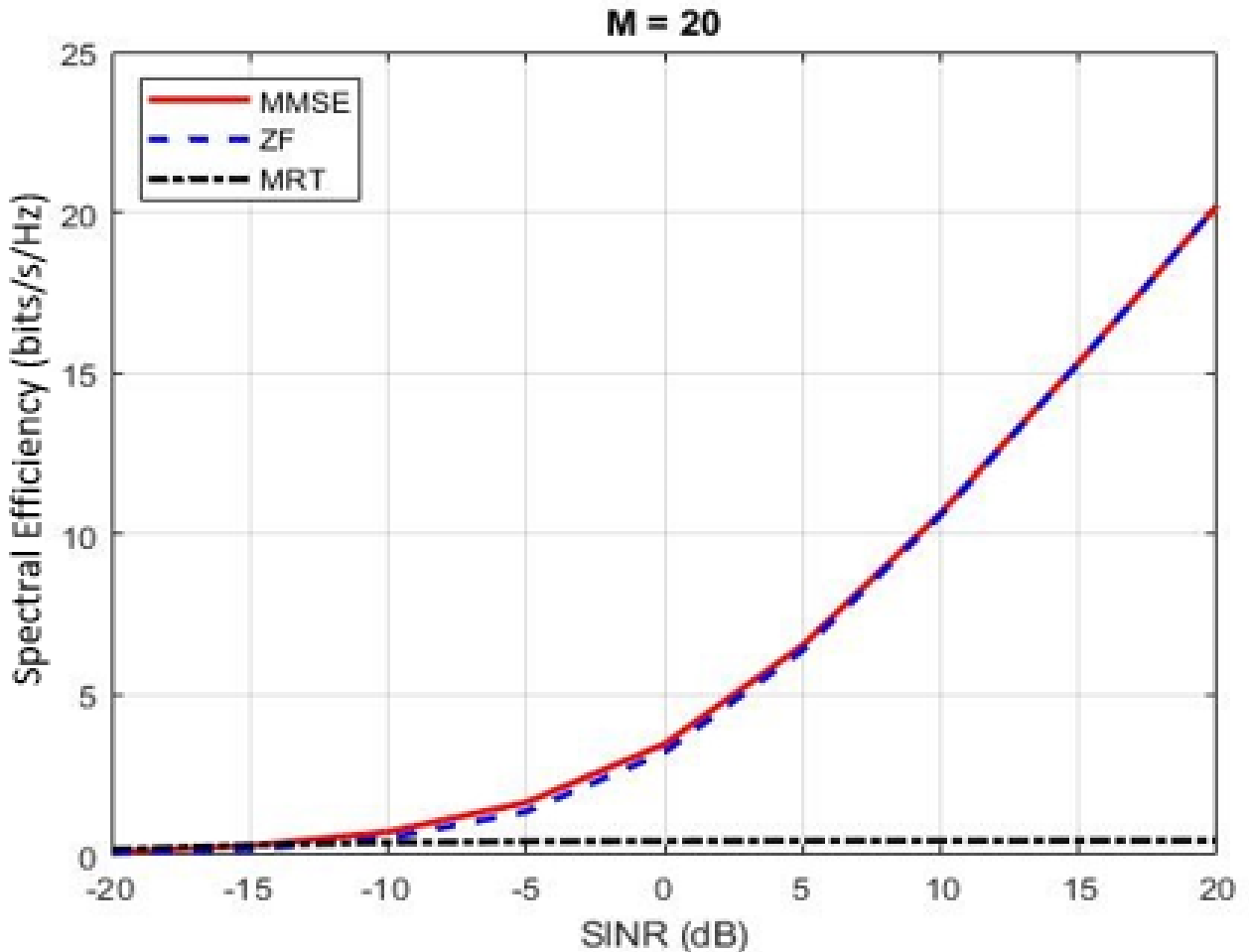


Figure 4.8: The achievable rate with different SINR for MMSE, ZF and MRT. $M = 20$, and $K = 10$ under no CSI

In this case, ZF performs worst among the three precoders in the low SNR region and a large portion of high SINR region (i.e. 0-15dB). For example, at 5dB, the

4.3. The Massive MU-MIMO Downlink System over Rayleigh Fading channel with no CSI at the transmitter

capacity using MMSE and MRT precoding are about 6bit/s/Hz and 2bit/s/Hz respectively whereas, capacity with ZF precoding is about 1bit/z/Hz. After -10dB, ZF again starts to perform better than MRT.

Figure 4.9 shows the achievable rate of users when we increase the number of antennas from 20 to 40. All results show that the system performance is improved. The achievable rates of MMSE, ZF, and MRT are increased by increasing the number of antennas. Corresponding to the results in Figure 4.8, MMSE gives the highest achievable rate to users. For comparison between ZF and MRT, ZF still gives the better performance at high SNR while MRT performs the higher rate at low SNR. We observe that a point, where ZF performance is better than MRT, is moved from -10 to -15 dB SNR. Increasing the number of antennas makes ZF able to be used at low SINR.

4.3. The Massive MU-MIMO Downlink System over Rayleigh Fading channel with no CSI at the transmitter

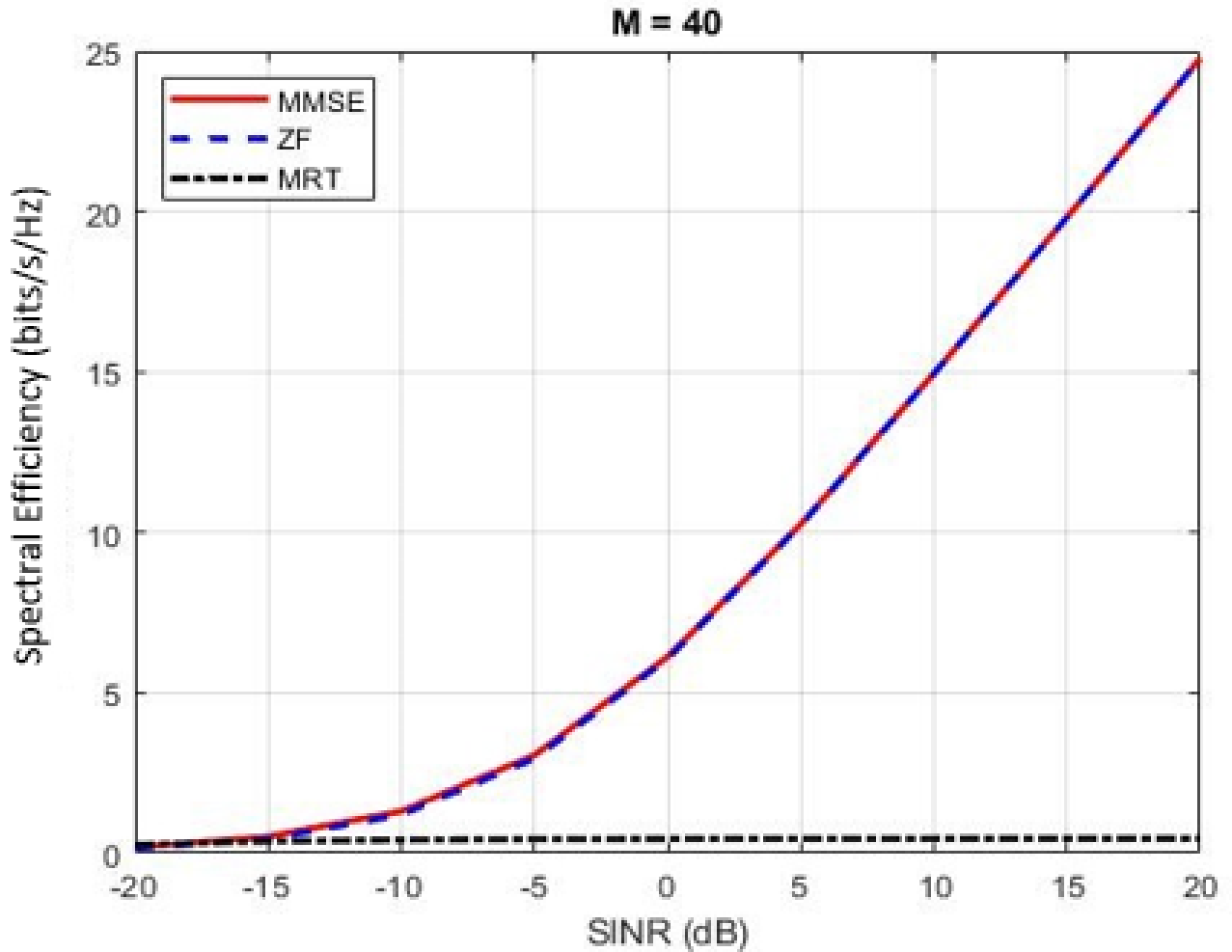


Figure 4.9: Same as Figure 4.8 but with $M = 40$

In case of variance = 0.3 assumption in Figure 4.10, the behaviour of the precoder is almost same as perfect CSIT condition shown in Figure 4.4, except the capacity in this case is slightly less. Here, MMSE and ZF performs better than MRT.

4.3. The Massive MU-MIMO Downlink System over Rayleigh Fading channel with no CSI at the transmitter

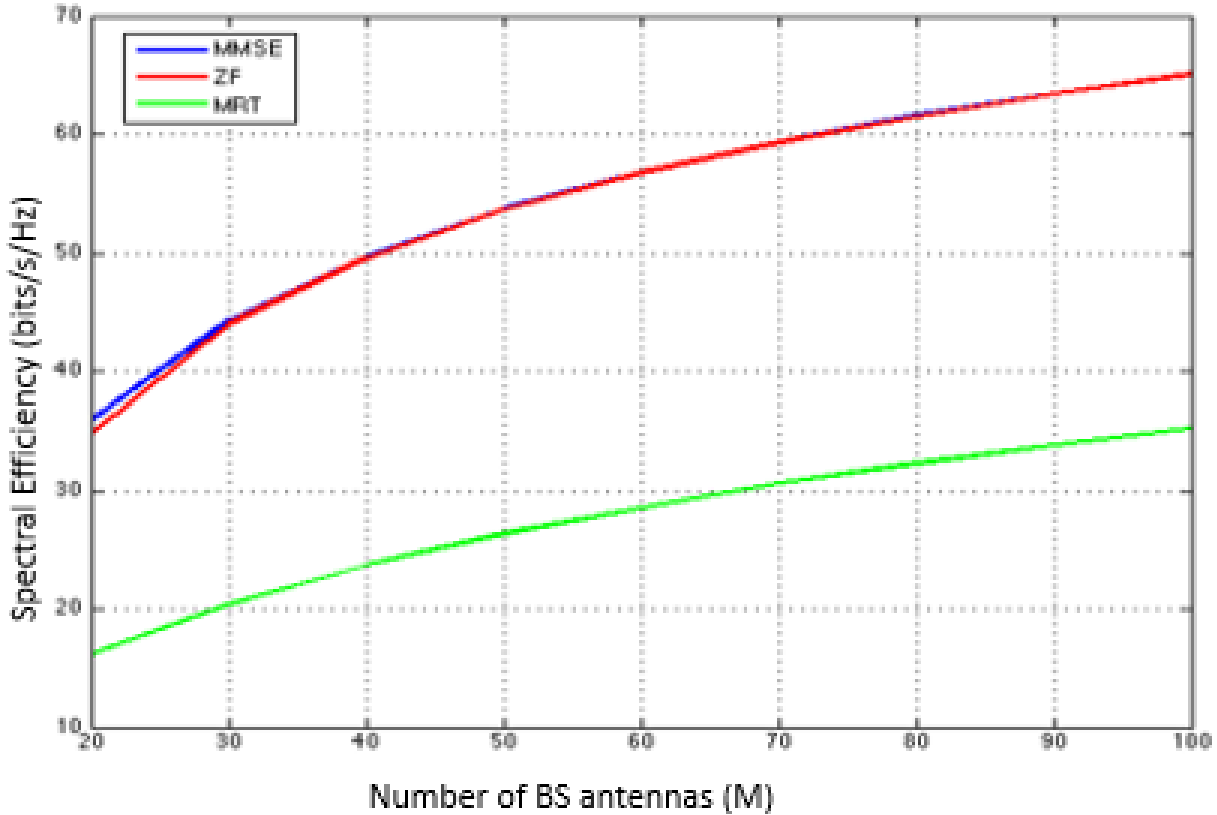


Figure 4.10: System capacity with the increase of the number of BS antenna under incomplete CSIT

4.3.2 Change in capacity with the increase of a number of user

In Figure 4.11 for the variance 0.3, It shows a similar pattern as perfect CSIT except for the decreased capacity. In this case, the performance of MRT precoding becomes close to MMSE and ZF. In other words, the performance of MRT is less affected by random assumption than ZF and MMSE.

4.3. The Massive MU-MIMO Downlink System over Rayleigh Fading channel with no CSI at the transmitter

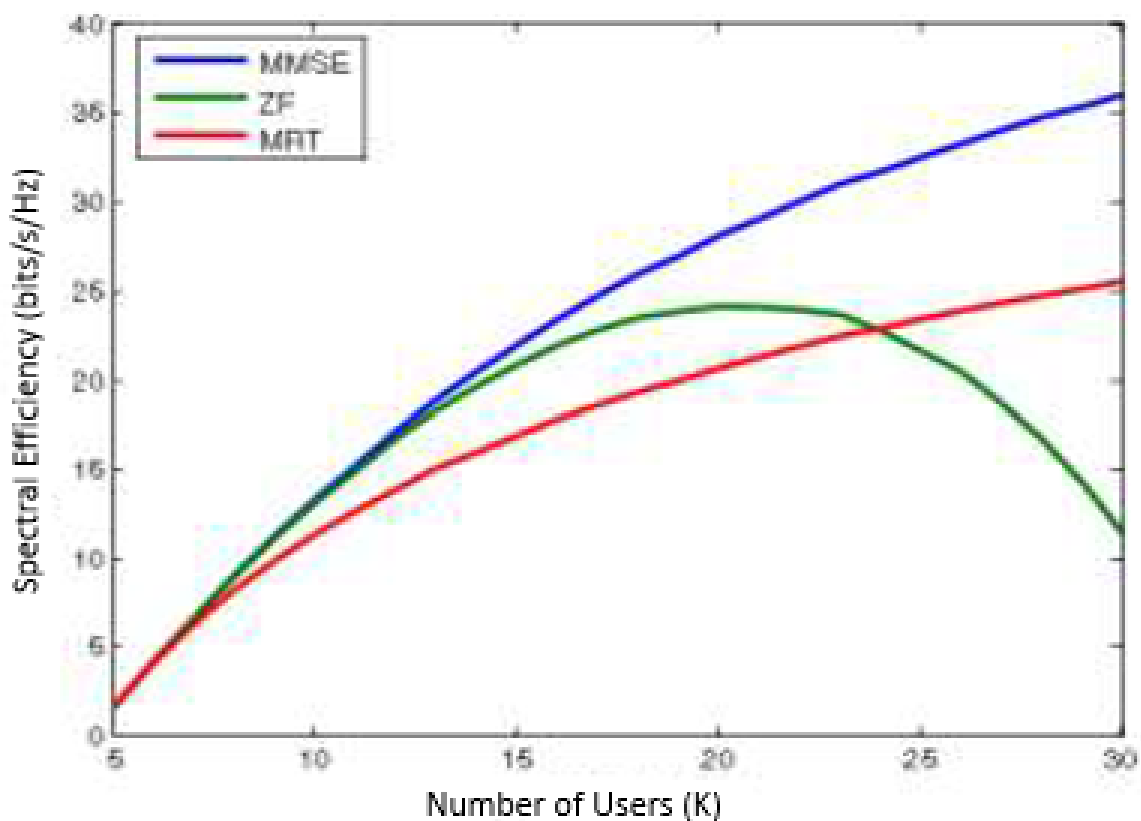


Figure 4.11: System capacity with the increase of the number of user under incomplete CSIT

Chapter 5

Conclusion and Future work

5.1 Conclusion

A massive MIMO system introduces the opportunity of increasing the spectral efficiency (in terms of bits/s/Hz) and improving the energy efficiency (in terms of bits/J) simultaneously. This system is able to use a simple processing such as MMSE, ZF, and MRT at the base station and using channel estimation from the uplink.

In this thesis, we have analysed and evaluating linear precoding for massive MIMO under both perfect CSI and Imperfect CSI. Due to imperfect CSIT, the capacity of all precoder falls than the capacity with perfect CSIT

Number of BS antenna is crucial to the performance. conversely, number of terminals antenna degrade the performance due to user interference. As the number of terminals increases the mathematical complexity of SINR increases. Generally, MRT gives lower complexity at high number of terminals while MMSE gives higher complexity.

Generally, ZF gives better performances at high transmission power while MRT gives better performance at the low transmission power. However, MMSE gives the best performance at low and high transmission power. Besides massive MU-MIMO can use a simple processing, the propagation environment does not affect much on the system performance.

Therefore, a massive MIMO system is a key in next wireless system. It presents advantages in terms of the achievable rate, the spectral efficiency, and the energy efficiency.

5.2 Recommendations for Future Work

Here are list of recommendations to the possible extensions of the works of this thesis research:

- Massive MIMO precoding schemes developed in this thesis consider only a one single cell wireless network. Further works can extend these schemes for a system with more than two cell (i.e. extend it to larger networks) which can improve the spectrum utilization efficiency.
- With a practical channel model without interference such as the Nakagami-m fading channel, the massive MIMO system with the linear precoding improves the performance with different parameters when the number of antennas was increased.
- Linear precoding is assumed at downlink transmission. Therefore it is desirable to study and incorporate adaptive transmit beamforming which is a key to increased spectral and energy efficiency in very large antenna arrays
- An orthogonal transmission strategy has been considered in this work which can impact the spectrum utilization efficiency; it would be beneficial to deal it with non orthogonal

References

- [1] Thomas L. Marzetta , Erik G. Larsson , Hong Yang , Hien Quoc Ngo "Fundamentals of Massive MIMO" Cambridge University Press, Institute of Education, on 25 Jan 2017
- [2] Larsson, Erik, Ove Edfors, Fredrik Tufvesson, and Thomas Marzetta, "Massive MIMO for next generation wireless systems," *Communications Magazine*, IEEE, vol. 52, no. 2, pp. 186-195, 2014.
- [3] Md. Mahfuzur Rahman, Dr.Md. Abu Bakar Siddiqui, "Performance Analysis of Massive MIMO with Different Precoders under Perfect and Imperfect CSIT Condition,". *International Journal of Engineering Trends and Technology (IJETT)*, - Volume 33 Number 1- March 2016
- [4] Adil Israr, Zahid Rauf,Jan Muhammad and Faisal Khan "Performance Analysis of Downlink Linear Precoding in Massive MIMO Systems Under Imperfect CSI". *Springer Science+Business Media New York*, 2017
- [5] Keke Zu, "Novel Efficient Precoding Techniques for Multiuser MIMO Systems," *Communications Research Group Department of Electronics*, University of York, May 2013.
- [6] Ehab ALI, Mahamod ISMAIL, Rosdiadee NORDIN, Nor Fadzilah ABDULAH, "Beamforming techniques for massive MIMO systems in 5G: overview, classification, and trends for future research" *Department of Electrical, Electronic and System Engineering*, Universiti Kebangsaan Malaysia (UKM), Bangi 43600, Malaysia, June 2, 2017
- [7] Eakkamol Pakdeejit, Hien Quoc Ngo,Dr. Daniel Persson, "Linear Precoding Performance of Massive MU-MIMO Downlink Sys-

- tem,". *in Sixth International Conf on Ubiquitous and Future Networks (ICUFN)*, Institutionen for system teknik Department of Electrical Engineering, Linkoping, 2013.
- [8] Selvan, V.P.; Iqbal, M.S.; Al-Raweshidy, H.S., "Performance analysis of linear precoding schemes for very large Multi-user MIMO downlink system,". *in Fourth International Conference on Innovative Computing Technology (INTECH)*, London, pp. 219-224, 13-15 August 2014.
- [9] Zhao, Long, Kan Zheng, Hang Long, and Hui Zhao, "Performance analysis for downlink massive MIMO system with ZF precoding,". *Transactions on Emerging Telecommunications Technologies*, vol. 25, no. 12, pp. 1219-1230, 2014.
- [10] Rusek, F., Persson, D., Lau, B. K., & Larsson, E. G. (2012). "Scaling up MIMO: Opportunities and challenges with very large arrays". *IEEE Signal Processing Magazine*, 30(1), 40-60.
- [11] Hoydis, J., Brink, S. T., & Debbah, M. (2013). "Massive MIMO in the UL/DL of cellular networks: How many antennas do we need?" *IEEE Journal on Selected Areas in Communications*, 31(2), 160 - 171.
- [12] Hoydis, J., Hoek, C., Wild, T., & ten Brink, S. (2012). "Channel measurements for large antenna arrays". *In International symposium on wireless communication systems (ISWCS)*, Paris (pp. 811 - 815).
- [13] Marzetta, T. L. (2015). "Massive MIMO: An introduction". *Bell Labs Technical Journal*, 20, 11 - 22.
- [14] Gao, X., Tufvesson, F., Edfors, O., & Rusek, F. (2012). "Measured propagation characteristics for very large MIMO at 2.6 GHz". *In Conference on signals, systems and computers (ASILOMAR)* (pp. 295 - 299).

-
- [15] Gao, X., Tufvesson, F., & Edfors, O. (2013). "Massive MIMO channels Measurements and models". *In Asilomar conference on signals, systems and computers, Pacific Grove, CA* (pp. 280 - 284).
- [16] Gao, X., Edfors, O., & Rusek, F. (2011). "Linear pre-coding performance in measured very-large MIMO channels". *In IEEE vehicular technology conference (VTC Fall)* (pp. 1 - 5).
- [17] Yang, H., & Marzetta, T. L. (2011). "Performance of conjugate and zero-forcing beamforming in large-scale antenna systems". *IEEE Journal on Selected Areas in Communications*, 31(2), 172 - 179.
- [18] Artigue, C., & Loubaton, P. (2011). "On the precoder design of Rayleigh fading MIMO systems equipped with MMSE receivers". *A large-system approach. IEEE Transactions on Information Theory*, 57(7), 4138 - 4155.
- [19] Appaiah, K., Ashikhminand, A., & Marzetta, T. L. (2010). "Pilot contamination reduction in multi-user TDD systems". *IEEE international conference on communications (ICC)*, pp.1 - 5.
- [20] ZM. Joham, K. Kusume, M. H. Gzara, W. Utschick, and J. Nossek, "Transmit wiener filter for the downlink of TDD DS-CDMA systems," *in Spread Spectrum Techniques and Applications*, 2002 IEEE Seventh International Symposium on, vol. 1, 2002, pp. 9-13 vol.1.
- [21] Huh, H., Caire, G., Papadopoulos, H. C., & Ramprasad, S. A. (2012). "Achieving massive MIMO spectral efficiency with a not-so-large number of antennas". *IEEE Transactions on Wireless Communication*, 11(9), 3226-3239.
- [22] Ashish Kumar, Ankit Aswal, Lalit Singh, "4G Wireless Technology" *International Journal of Engineering and Management Research*, Volume-3, Issue-2, April 2013, 30(1), 35-43

- [23] Yang, H., & Marzetta, T. L. (2013). "Performance of conjugate and zero-forcing beamforming in large-scale antenna system". *IEEE Journal on Selected Areas in Communications*, 31(2), 172 - 179.
- [24] Ngo, H. Q. (2015). "Massive MIMO: Fundamentals and system designs". *Ph.D. thesis, Department of Electrical Engineering, Linkoping University*.
- [25] Athanasios Papoulis, s. Unnikrishna Pillai & Venkatesan, S. (2012). "PROBABILITY, RANDOM VARIABLES, AND STOCHASTIC PROCESSES". *North America: McGraw-Hut*. fourth edition, 2002
- [26] Utschick, W., & Josef, A. (2005). "Linear transmit processing in MIMO communications systems". *IEEE Transactions on Signal Processing*, 53(8), 2700-2712.
- [27] Tse, D., & Viswanath, P. (2004). "Fundamental of wireless communications". *Cambridge University Press*. ISBN-10: 0521845270.